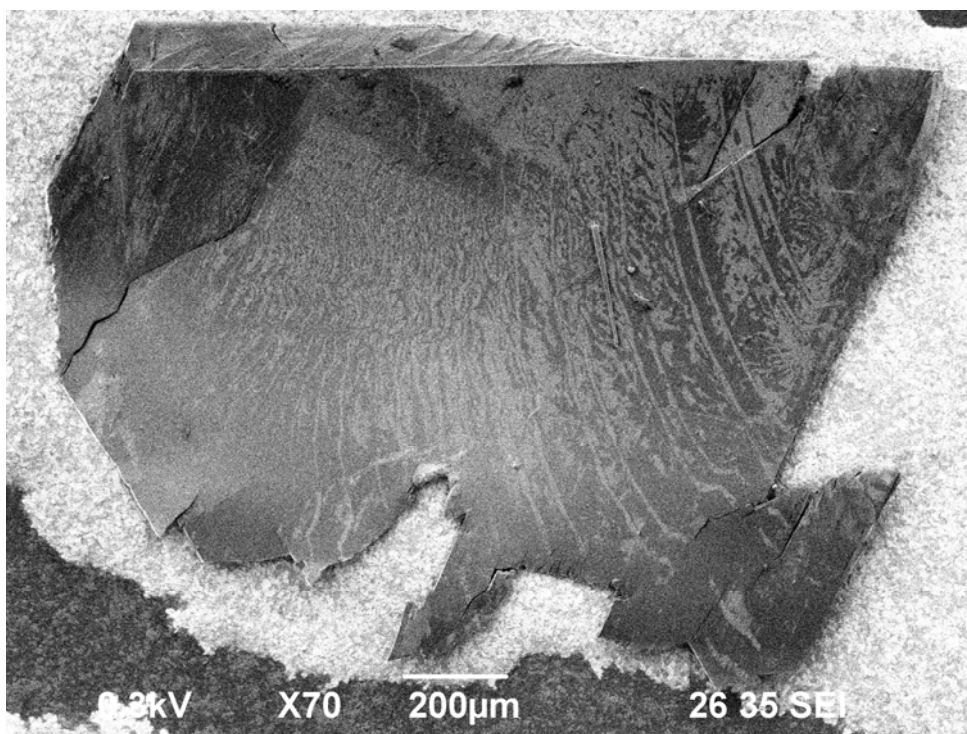


Electrical characterization of pentacene single-crystal devices



Master thesis
Enschede, 26 January 2010

Adit Pradhana Jayusman
s1000810
Master student of Chemical Engineering, Molecules and Materials track
University of Twente

Electrical characterization of pentacene single-crystal devices

Master student

Adit Pradhana Jayusman

s1000810

Master student of Chemical Engineering, Molecules and Materials track

Graduation committee

Prof. Dr. ing. D.H.A. Blank

Ir. P.J. de Veen

Dr. P.M. Schön

Dr. ing. A.J.H.M. Rijnders

Institution

Inorganic Materials Science

Faculty of Science and Technology

MESA+ Institute of Nanotechnology

University of Twente

The Netherlands

The figure on the front page shows the pentacene single-crystal surface. The light grey irregular shaped patches are the 6,13-pentacenequinone layers. The image was taken by SEM in low acceleration voltage mode (0.3 kV).

Abstract

Pentacene is one of the most popular and well-studied organic semiconductor materials. Pentacene also has become the model for studying the physical properties of molecular organic semiconductor materials. To study the intrinsic electronic properties and to explore the physical limits of pentacene, focusing on the fabrication of devices, such as organic field-effect transistor (OFET), based on pentacene single-crystal seems to be the best approach.

Pentacene is known to slowly oxidize in the presence of air and light. The oxidation product, 6,13-pentacenequinone (PQ), is concentrated on the pentacene single-crystal surface. The presence of PQ layer will decrease the electrical properties of pentacene based FET by increasing the charge injection resistance in pentacene/electrode and pentacene/dielectric interfaces. Recently, it has been found that the PQ layer can be removed selectively by using SEM-monitored *in-situ* surface heat treatment.

Here, we have performed *in-situ* heat treatment with SEM monitoring to remove the PQ layer from the pentacene single-crystal surface. This method has several weaknesses. However, this method is applicable to study the PQ layer removal qualitatively. We also have been able to obtain lower limit intrinsic mobility (μ) values of pentacene single-crystal from the I - V curves of simple space-charge-limited current device. Nevertheless, we found that the μ values that we have got are much smaller than the values that have been reported in literatures.

Keyword: Pentacene single-crystal, 6,13-pentacenequinone, *in-situ* heat treatment, hole mobility.

Acknowledgements

Well, this is the end of my pursuit of master level knowledge in the Netherlands, and I am still alive! Although I only stayed in the Netherlands for one year, I have experienced a lot on many accounts. Luckily, I was not alone during this period. There were so many fantastic people that I encountered. Had not it been for pursuing the MSc degree at the University of Twente, I would not have got the opportunity to meet them.

This thesis is the result of six months work in the Inorganic Materials Science lead by Dave Blank at the University of Twente.

I would like to express my gratitude to Ben Betlem and Rik Akse for giving me the opportunity to join this challenging Double-Degree Program. I also would like to thank Indra Noviandri and Desy Natalia of Institut Teknologi Bandung for their help during the selection process.

I would like to thank the people who greatly helped me in accomplishing this project. First of all, I would like to express my gratitude to Guus Rijnders for giving me the opportunity to work in this project, and for his kindly guidance and encouragement throughout the past twelve months. Next, I thank Peter de Veen for his good mentoring and fruitful discussion. I also thank Frank Roesthuis for his help during my research in MESA⁺. I also thank to all great people in the IMS group for their support during my research and my fellow IMS-students: Maarten, Sandra, Wouter, Rogier, Enne, Bouwe, Arjan, Peter, Herman, and Rik, thanks for sharing the office with me. Furthermore, I would like to thank to Dave Blank and Peter Schön for being my graduation committee.

I would like to thank to all my Indonesian friends in Enschede and all of the members of UT-Moslems community for their warm friendship during my stay at Enschede. I also would like to thank my family in Enschede, Oom Jaap, Tante, Elli, and Elsera for their support. Last but not least, I want to thank to my parents, my sister, my grandparents, and all of my family for their moral support throughout my study. Finally, I would to express my sincerest gratitude to the Almighty God.

Enschede, January 2010

Adit Pradhana Jayusman Setyogroho

Table of Contents

Abstract	ii
Acknowledgements	iii
Table of Contents	iv
Chapter 1 Introduction.....	1
1.1 Aim of research.....	2
1.2 Outline.....	3
Chapter 2 Theoretical Backgrounds	4
2.1 Organic semiconductors.....	4
2.1.1 Basic properties of organic semiconductors	6
2.1.2 Charge transport in organic semiconductor.....	6
2.1.3 Charge carrier in organic semiconductor.....	8
2.2 Pentacene.....	11
2.2.1 Crystal growth of pentacene.....	15
2.2.2 Pentacene single-crystal	16
2.2.3 Pentacenequinone on pentacene single-crystal surface	16
2.3 Space-charge-limited current	18
Chapter 3 Experimental	22
3.1 Equipments	22
3.1.1 Nanomanipulator system	22
3.1.2 Heater set-up.....	22
3.1.3 Pulsed laser deposition system	23
3.2 Pentacene single-crystal surface characterization.....	23
3.2.1 Sample preparation.....	23
3.2.2 SEM characterization.....	23
3.2.3 <i>In-situ</i> heat treatment.....	23
3.3 Electrical characterization of pentacene single-crystal device.....	24

Chapter 4	Results and Discussion	26
4.1	Pentacene single crystal surface.....	26
4.1.1	SEM characterization.....	26
4.1.2	<i>In-situ</i> heat treatment.....	27
4.2	Electrical characterization of pentacene single-crystal device.....	29
4.3	Discussion.....	33
Chapter 5	Conclusion and Suggestions	34
5.1	Conclusion.....	34
5.2	Suggestions	34
References	36

Chapter 1 Introduction

Since the invention of the transistor on 23rd December 1947 by Walter Brattain and John Bardeen (members of William Shockley group) [1], silicon is the material of choice for the fabrication of high-performance semiconductor devices. The last decades, however, the field of organic electronics has emerged and gained considerable interest. The first complete organic field-effect transistor (polythiophene field-effect transistor) –the fundamental component in electronic devices– is reported in literature in 1987 [2, 3].

In organic electronics, the inorganic components in the device are replaced by organic semiconductor material. The use of these organic materials to build electronics seems most attractive in the fabrication of low-cost applications, especially when cheap printing techniques can be used on a large area and/or on flexible substrates. Displays based on organic LEDs (light emitting diode) [4, 5] and organic RFIDs (radio-frequency identification device) [6, 7] have already made their way into the commercial market. Also much research is performed the last years on low-price organic solar cells [8] and e-paper [9, 10].

Not only useful in practical applications, organic semiconductor materials also gained considerable interest in research, to unfold the relation between their electronic and crystal structure with their intrinsic properties, mainly their transport properties. There is also much room for theoretical development in this field [11]. Organic single-crystals are used as tools for the exploration of charge transport phenomena in organic materials because of their high purity and similarity to the single-crystal structures of inorganic electronics [12]. Nevertheless, the single-crystal systems are more complex than was imagined by the researchers, as mentioned by Jurchescu *et al.* [13].

Among the organic semiconducting materials, pentacene is one of the most popular and well-studied material. Pentacene also has become the model for studying the physical properties of molecular organic semiconductor materials [11, 14, 15]. The use of pentacene single-crystals in fundamental research field increased remarkably in the last decade, especially to study their intrinsic electronic properties [13].

To study the intrinsic electronic properties and to explore the physical limits of pentacene, focusing on the fabrication of devices, such as organic field-effect transistor (OFET), based on pentacene seems to be the best approach [16-20].

In pentacene thin-film transistors, the electrical properties of pentacene thin-films are influenced by many parameters, such as bulk purity and structural defects. Defects in pentacene thin-films can be classified into intrinsic and extrinsic defects. Intrinsic properties of pentacene thin-films can be seen as the nature of the pentacene thin-films itself, apart from external factors. The presence of external factor, extrinsic defects, will cause the pentacene thin-film devices to exhibit different behavior from its nature (intrinsic properties). This behavior can be seen as the extrinsic properties of pentacene thin-films. That is why the thin-film transistors are not suitable for the study of intrinsic electronic properties of pentacene, because their characteristics are often strongly affected by imperfection in the film structure and by the low purity of the pentacene itself. Thus, as mentioned before, to explore the intrinsic electronic properties of pentacene, FETs based on single-crystal of pentacene are more suitable.

1.1 Aim of research

The long-term goal of this research is to understand about the fundamental properties of pentacene by fabrication and characterization of pentacene single-crystal field-effect transistor devices.

Pentacene is known to slowly oxidize in the presence of air and light. The oxidation product, 6,13-pentacenequinone, is concentrated on the pentacene single-crystal surface. Recently, it has been found that the oxidized material can be selectively removed by a surface treatment. This procedure enables an *in-situ* cleaning of the pentacene crystal surface before fabricating the field-effect devices. However, the influence of this treatment on the electrical properties of fabricated devices is still unclear.

In this research, we hypothesize that the presence of 6,13-pentacenequinone layer on pentacene single-crystal surface will decrease the electrical properties of pentacene based FET by increasing the resistance for charge injection from the electrode through the pentacene and pentacene/dielectric interface, as in a FET the conducting channel will be formed there. Thus, by removing the 6,13-pentacenequinone layer, increasing of electrical properties (in this case hole mobility) will be expected.

Therefore, to clarify the relation between 6,13-pentacenequinone presence on pentacene single-crystal surface with pentacene intrinsic electronic properties, we have two aims in this research. First, a systematic study will be performed to remove the 6,13-pentacenequinone and second, the

influence of the removal on the electrical transport properties (in this case hole mobility) of pentacene single-crystal devices will be studied. The latter aim will be studied through simple space-charge-limited current devices fabricated with and without performing surface treatment.

1.2 Outline

Theoretical backgrounds are explained in Chapter 2. The theoretical backgrounds consist of a brief introduction to organic semiconductor, pentacene system, and the space-charge-limited current. Details about the experiments (equipments and procedures) are explained in Chapter 3, followed by the result of these experiments and the discussion in Chapter 4. Conclusion and suggestions are presented in Chapter 5.

Chapter 2 Theoretical Backgrounds

2.1 Organic semiconductors

Organic semiconductors are generally divided into two major classes, low molecular weight (small) molecules and polymers made from a small foundational group of conjugated monomer units, shown in Figure 2.1.

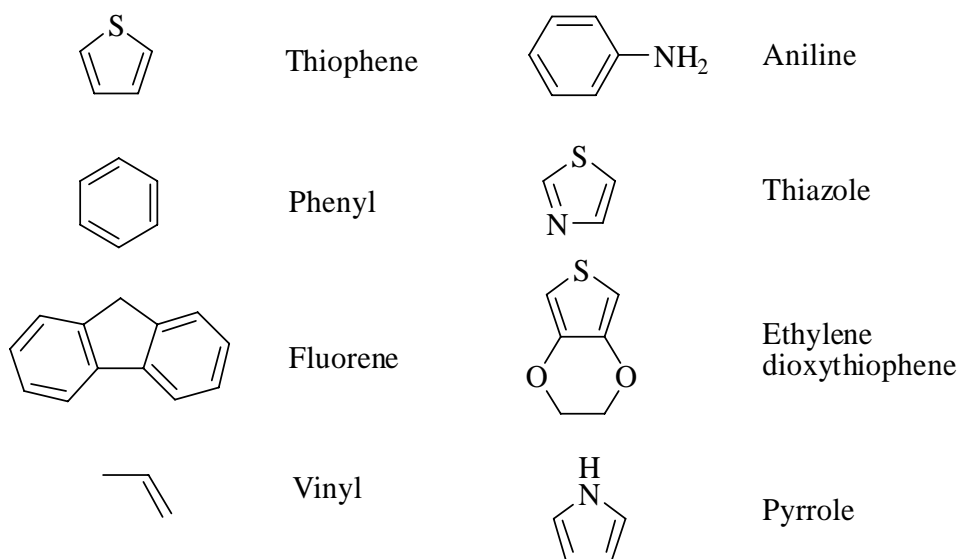


Figure 2.1. Some of the more common repeating functional units in conjugated organic materials. Most organic semiconductors and conductors are made from fused or linked elements like these, which are rich in sp^2 -hybridized carbon atoms and delocalized π -electrons.

The common structural feature in organic semiconductors is the presence of a conjugated backbone of alternating single and double bonds. From molecular physics, it has been known that the so-called double bond between two carbon atoms can be formed due to a sp^2 -hybridisation: three degenerate orbitals are constructed out of one s and two p orbitals. They are co-planar and oriented at 120° relative to one another. Chemical bonds formed by these orbitals are called as σ bonds (single bonds); they are localized between the bonding C atoms. The fourth orbital, p_z remains unchanged and is directed perpendicular to the plane of the sp^2 orbitals, and thus to the plane of C atoms.

The p_z orbitals of neighboring atoms overlap. This leads to an additional bond, the so-called π bond (double bond), and to delocalized density of electrons above and below the plane of the molecule. This is the nodal plane for the π -electron density. Figure 2.2 (left panel) shows images of σ and π bonds in ethene.

As compared to the σ bonds forming the backbone of the molecules, the π bonding is significantly weaker. Therefore, the lowest electronic excitations of conjugated molecules are the π - π^* transitions (see Figure 2.2, the right panel).

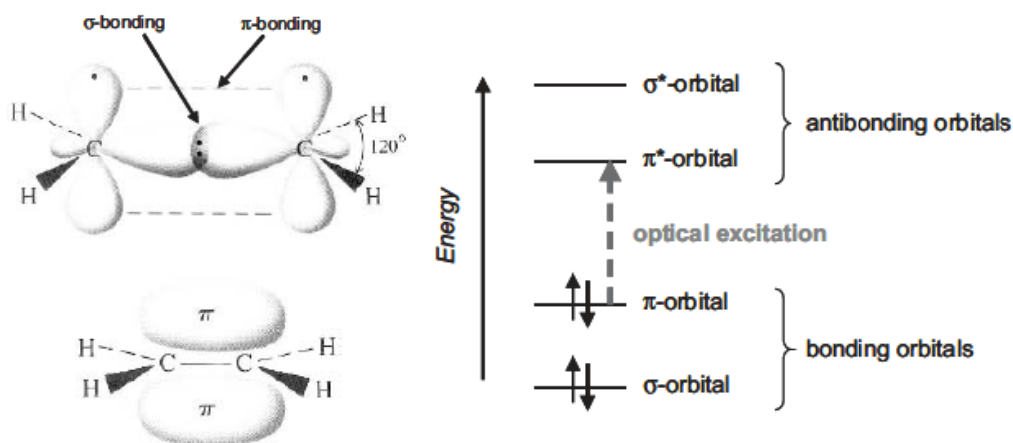


Figure 2.2. Left panel shows images of σ and π bonds in ethene, as an example for the simplest conjugated π -electron system. Right panel shows the energy levels of a π -conjugated molecule. The lowest electronic excitation is between the bonding π -orbital and the anti-bonding π^* -orbital. Bonding orbitals and anti-bonding orbitals are also known as highest occupied molecular orbitals (HOMO) and lowest unoccupied molecular orbitals (LUMO), respectively. Reproduced from [21].

The HOMO-LUMO gap of organic semiconductors is in the range of 1-4 eV [22]. Thus, it can be said that organic semiconductors are wide band-gap semiconductors. From the large band-gap, we might expect that organic materials are insulator. Thus, a large thermal energy must be acquired by electron in order to jump from the valence band to the conduction band. However, there are some effective methods that can be used to generate charge carriers in the organic semiconductors: injection of carriers from metallic electrodes; optical excitation, created hole-electron pair; field-effect doping; and electrostatic or chemical doping. An illustration of optical excitation is shown in Figure 2.2. Charge carrier generation by chemical doping also described in Chapter 2.1.3. Injection of carriers from metallic electrodes is the method that was used in this work to generate charge carriers.

An important difference between the two classes of materials lies in the way of how they are processed to form thin-films. Whereas small molecules are usually deposited from gas phase by sublimation or evaporation, conjugated polymers can only be processed from solution *e.g.* by spin-

coating or printing techniques. Additionally, a number of low molecular materials can be grown as single-crystals (*e.g.* pentacene) allowing intrinsic electronic properties to be studied on such model systems.

2.1.1 Basic properties of organic semiconductors

The nature of bonding in organic semiconductors is fundamentally different from their inorganic counterparts. Organic molecular crystals are van der Waals bonded solids. The van der Waals bonding is considered to be weaker compared to covalent bonding. Therefore, the organic molecular crystals have weaker intermolecular bonding compared to covalently bonded semiconductors like GaAs or Si. As a result, the mechanical and thermodynamic properties of organic molecular crystals, such as hardness and melting point, will be inferior to the inorganic counterparts (the organic molecular crystals possess reduced hardness and lower melting point). More importantly, organic molecular crystals have a much weaker delocalization of electronic wave functions among neighboring molecules. This has direct implications for charge carrier transport and optical properties. The situation in polymers is somewhat different since the morphology of polymer chains can lead to improved mechanical properties. However, the electronic interaction between adjacent chains is usually also quite weak in this class of materials.

The conjugation systems in organic semiconductors held an important role in the charge carrier transport process. The simplest conjugation system can be seen in polyethyne (also known as polyacetylene). The discovery of I₂-doped polyacetylene (see Figure 2.3), which is far more conductive than the pure state polyacetylene, by Shirakawa and co-workers [23] is the major breakthrough in organic electronic field. This led to a large increase of research in organic semiconductors field.

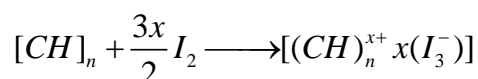


Figure 2.3. Polyacetylene is transformed into a metallic conductor by doping. Electron acceptors, in this case iodine, oxidize the polymer. The electrons are taken away from the filled lower band of polyacetylene and used to form the iodide ions, leaving holes, which result in a *p*-type material.

2.1.2 Charge transport in organic semiconductor

Polyacetylene will be used as a model to explain charge transport in this section. In a polyconjugated system, the π -orbitals are assumed to overlap, and form a valance and a conduction band as predicted by band theory. If all of the bond lengths were equal, *e.g.* delocalization led to each bond having equal partial double bond character, then the bands would overlap and the polymer would behave like a quasi-one-dimensional metal, having a good conductivity. However, a linear chain of

equispaced atoms in a metal, such as a chain of sodium atoms, is found to be an energetically unstable system and will undergo lattice distortion by alternative compressions and extensions of the chain. This leads to alternating atom pairs with long and short interatomic distances found along the chain. This variation in spacing is called as Peierls distortion. Chemically, the Peierls distortion can be interpreted as an alternating of single (σ) and double (σ and π) bonds along the chain. The double bonds obviously are the short interatomic distance. The Peierls distortion makes the energy gap opens at the Fermi level, which will form valence band and conduction band. This break in the continuity of energy band is caused by the use of elastic energy during lattice distortion, which is compensated by lowering the electronic energy and formation of a band gap. A simple illustration of this explanation can be seen in Figure 2.4.

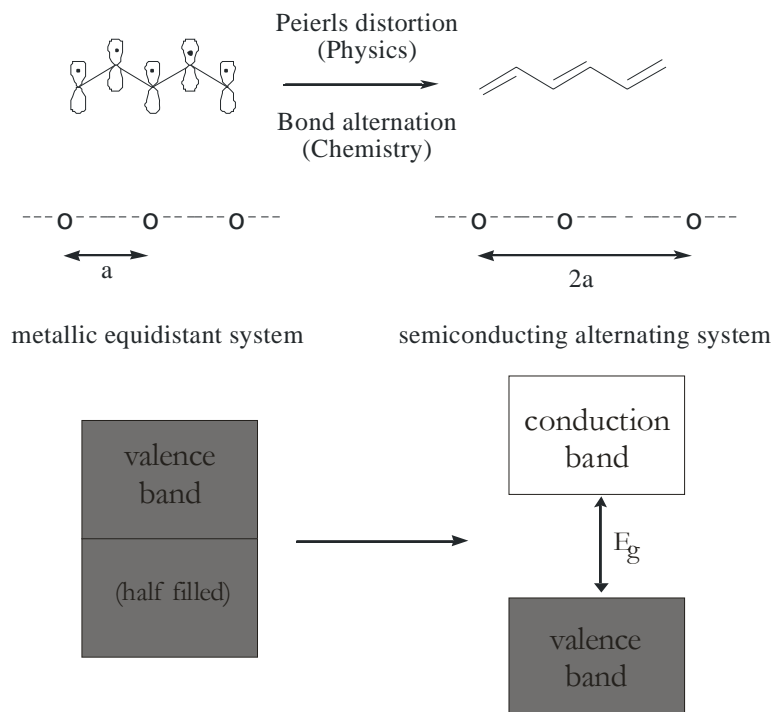


Figure 2.4. Schematic diagram illustrating the Peierls distortion that leads to the formation of energy gap and production of semiconductor rather than a conductor. Adapted from [24].

At the zero Kelvin, the energy level of electrons with the highest energy will be at the Fermi level, which lies in the band gap. There are no electron transport at zero Kelvin in semiconductors because no molecular state present at the band gap. At temperature above zero Kelvin, the number of thermally excited electrons that transferred from valence band to conduction band increases. Both of the electrons in conduction band (n -type) and the holes in valence band (p -type) give contribution to the transport of charge in the ideal material. At room temperature, only small number of electrons that thermally excited into the conduction band, given a free electron concentration of n .

These kinds of materials show an intrinsic electrical conductivity that lies between insulators and conductors: a semiconductor material.

Electrical conductivity is a function of the number of charge carrier species “ i ” (n_i), the charge of each carrier (e_i), and carrier mobilities (μ_i), described by Equation 2.1. Carrier mobility is a property that indicates how easy the charge accelerated through the lattice by an applied electric field.

$$\sigma = \sum \mu_i n_i e_i \quad \text{Equation 2.1}$$

In principle, the organic conjugated materials exhibit both n -type and p -type conductivity. However, most organic semiconductors only exhibit hole conductivity (p -type conductivity) because electron conductivity is suppressed by the electron traps. Charge traps happen at defects such as impurities in grain boundaries or at the interface between the electrodes.

2.1.3 Charge carrier in organic semiconductor

Conventional inorganic semiconductors have several important differences with their organic counterparts. The most notably difference is the charge carrier species. In conventional inorganic semiconductor, charges are fully delocalized and do not significantly distort their surroundings lattice. While in organic semiconductors, electrons and holes are only delocalized in a part of conjugation length (see Figure 2.5). Disorder determines the effective conjugation length in polymeric semiconductors [25].

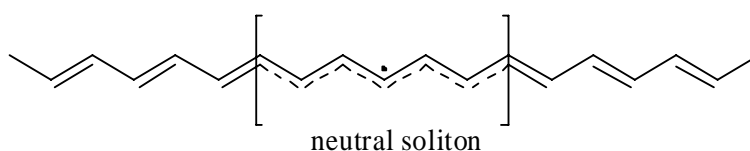


Figure 2.5. *Trans*-polyacetyleneconjugation system. The charge delocalization is shown inside the bracket. In this case, the neutral soliton acts as the charge species. Left and right region of polyacetylene are two degenerated ground state.

In polyacetylene, the *trans* structure of polyacetylene has a twofold degenerate ground state in which they are a mirror image and the single and double bonds can be interchanged without changing the energy (see Figure 2.5). The right sequence may form and eventually meet the left sequence, producing a free radical (neutral soliton). This neutral soliton breaks the pattern of bond alternation, it separates the generate ground state structures. The electron has unpaired spin (free radical) and is located in a non-bonding state in the energy gap, midway between the two bands. The presence of this neutral soliton gives the *trans*-polyacetylene a semiconductor characteristics and the

neutral soliton itself acts as the charge carrier species. Further processes (*e.g.* doping) will increase the conductivity of *trans*-polyacetylene. Different solitons will be formed, depends on the doping agent. An acceptor or *p*-doping agent, such as I_2 or $HClO_4$, removes an electron and creates a positive soliton or a neutral one if the removed electron is not the free radical. Similarly, a negative soliton can be formed by introducing a donor or *n*-doping agent that adds an electron to the mid-gap energy level (see Figure 2.6 for the structural details of solitons). The soliton defects only supported in a structure that possesses degenerated ground state [26].

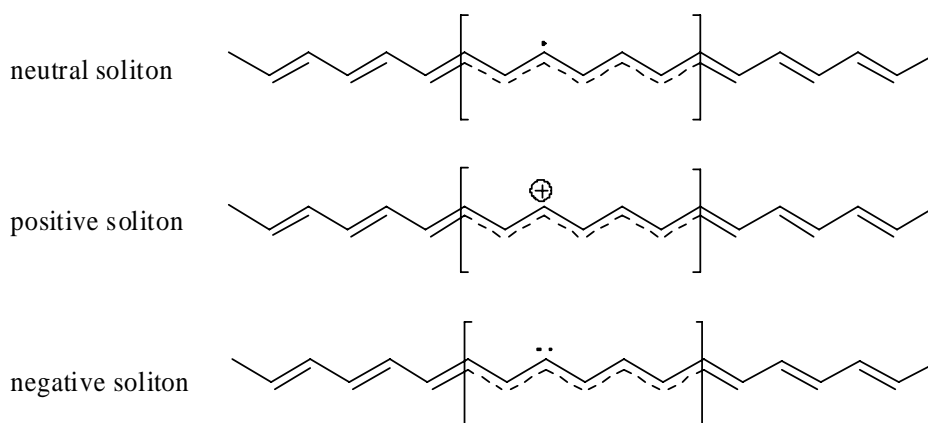


Figure 2.6. Different type of solitons: neutral soliton, positive soliton, and negative soliton. In chemical term, neutral soliton is a free radical, positive soliton is a carbocation, while negative soliton is a carbanion.

Another charge carriers in organic semiconductors are polaron and bipolaron. To explain this, poly(*p*-phenylene) will be used as the model.

As mentioned before, soliton defects only supported in a structure that possesses degenerated ground state. Thus, soliton defect cannot be supported in poly(*p*-phenylene) as there is no degenerated ground state. Instead, the two nearly equivalent structures are the benzenoid and quinoid forms, which have different energy level (see Figure 2.7).

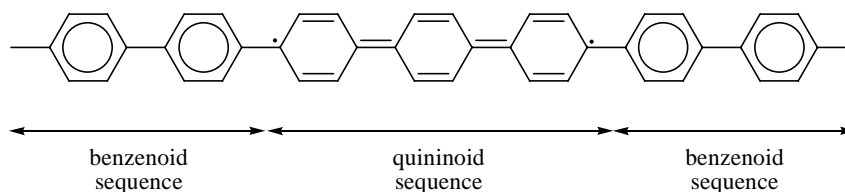


Figure 2.7. Poly(*p*-phenylene) chain. The benzenoid regions have a lower energy than quinoid region, which must be limited by the benzenoid structures.

In the band theory model, it is assumed that conduction appears because the mean free path of charge carrier extends over a large number of lattice sites, and the residence time on any site is small

compared to the time it would take for a carrier to become localized. However, if a carrier is trapped, it tends to polarize the local environment, which relaxes into a new equilibrium state. This deformed section of the lattice (the polarized local environment) and the charge carrier will form a species called polaron. Unlike the soliton, polaron is unable to move without overcoming an energy barrier. Thus, it will move in hopping motion.

In the poly(*p*-phenylene), the solitons are trapped by the changes in polymer structure because of the differences in energy. Thus, polaron is created, which is an isolated charge carrier. A pair of polarons is called as bipolaron. In poly(*p*-phenylene) and most of the other polyconjugated conducting polymers, the conduction occurs via polaron or bipolaron. Illustration of polaron and bipolaron can be seen in Figure 2.8. The formation of bipolaron bands in *p*-type polymer is also shown in Figure 2.8.

In molecular organic crystal, polaron acts as the charge carrier. In an organic molecular solid, the charge carrier transport is depending on the degree of order. It can fall between two extreme cases: band or hopping transport. Band transport is typically observed in highly purified molecular crystals at not too high temperatures. However, since electronic delocalization is weak, the bandwidth is only small as compared to inorganic semiconductors. Therefore, room temperature mobilities in molecular crystals only reach values in the range of 1 to 10 cm² V⁻¹ s⁻¹ [27]. As a characteristic feature of band transport, the temperature dependence follows a power law behavior.

$$\mu \propto T^{-n}, \text{ with } n = 1 \dots 3 \quad \text{Equation 2.2}$$

In other extreme case of an amorphous organic solid, hopping transport prevails, which leads to much lower mobility values (at best around 10⁻³ cm² V⁻¹ s⁻¹). Instead of a power law, the temperature dependence then shows an activated behavior and the mobility (μ) also depends on the applied electric field (F).

$$\mu(F, T) \propto \exp(-\Delta E / kT) \cdot \exp(\beta \sqrt{F} / kT) \quad \text{Equation 2.3}$$

As an example, band transport acts as charge carrier transport in pentacene single-crystals. The mobility increases with decreasing temperature with $n = 2.38$ [28].

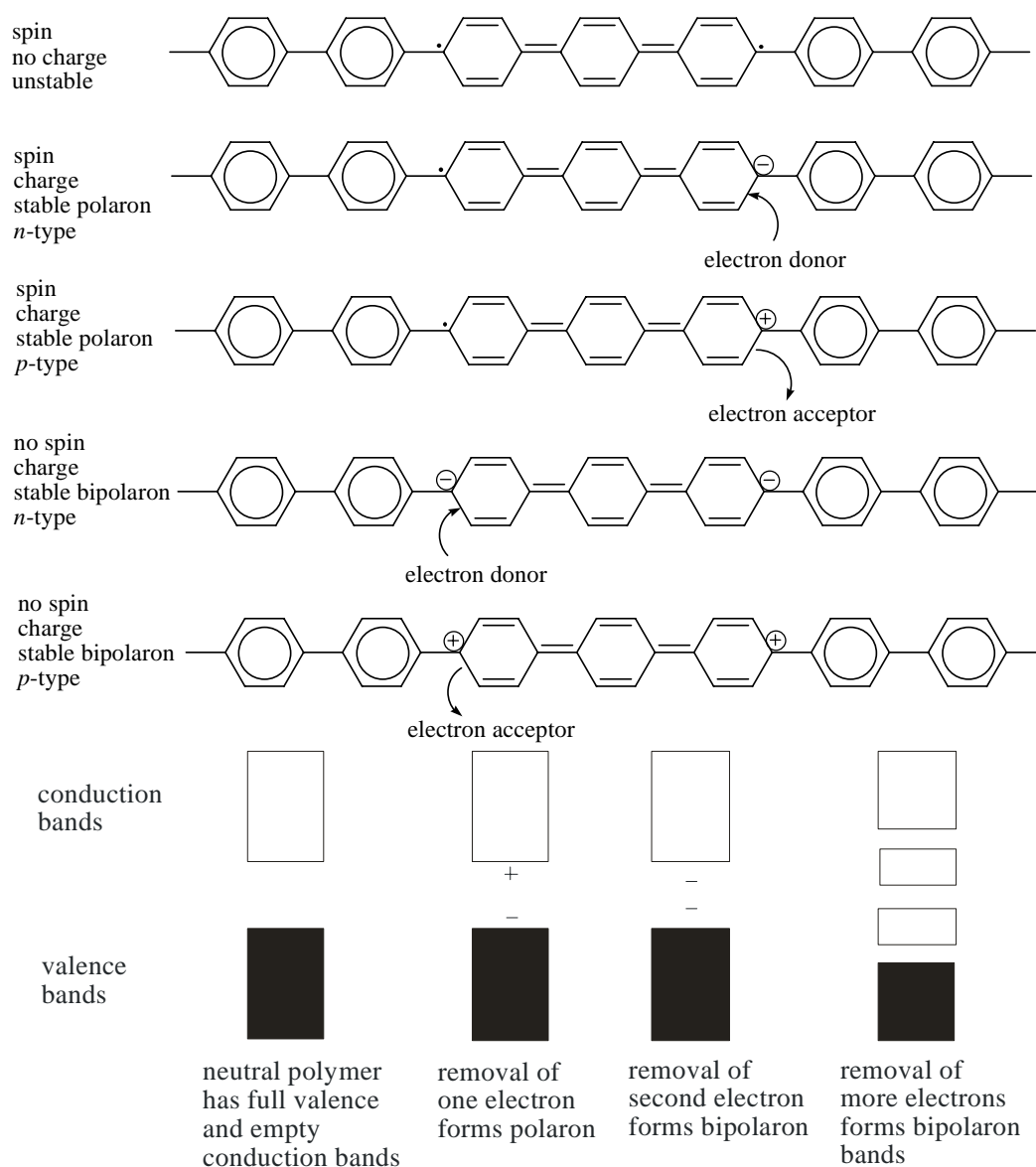


Figure 2.8. Illustration of polaron and bipolaron structure in poly(*p*-phenylene) and the proposed band structure for the oxidized polymer (*p*-type).

2.2 Pentacene

Pentacene, a polycyclic aromatic hydrocarbon compound, is a planar molecule made of five linearly fused benzene rings. The Lewis structure of pentacene is shown in Figure 2.9. Interest in pentacene has grown dramatically in recent years due to the fact that its crystals and thin films behaving as a *p*-type organic semiconductor, which can be employed to fabricate organic electronic devices, such as organic field-effect transistor (OFET) [17, 18, 29-36].

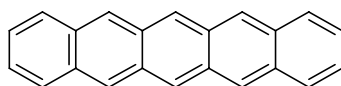


Figure 2.9. The Lewis structure of pentacene.

Pentacene and some of its derivatives were synthesized for the first time by William Hobson Mills and Mildred Mills in early 1912 [37]. They used pyromellitic anhydride and benzene as the starting materials. The reaction carried out in the presence of AlCl_3 as catalyst. The product from this reaction is an isomeric mixture of dibenzoyl-benzene-dicarboxylic acid. Upon heat treatment in concentrated sulfuric acid, dibenzoyl-benzene-dicarboxylic acid underwent an intermolecular condensation reaction by losing two water molecules, formed a dinaphthanthradiquinone. The intermolecular condensation reaction is shown in Figure 2.10. After dinaphthanthradiquinone formed, pentacene ($\beta,\beta,\beta',\beta'$ -dinaphthanthracene) could be obtained simply from the reduction of the diquinone groups. Another synthesis methods, which is more efficient, were suggested later on by Allen and Gates in 1943 [38].

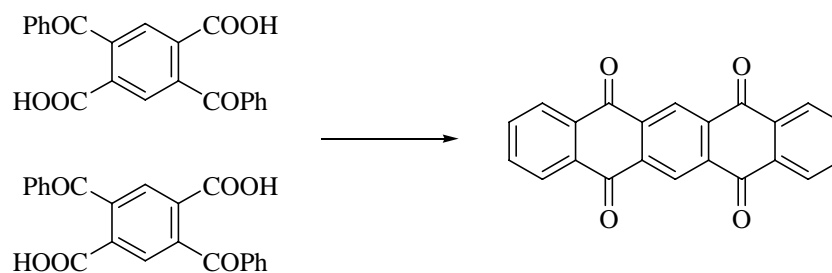


Figure 2.10. Intermolecular condensation reaction of two dibenzoyl-benzene-dicarboxylic acid molecules, which lead to formation of dinaphthanthradiquinone.

Modern synthesis methods have been invented in order to overcome the low solubility of pentacene in common organic solvents, which limits its deposition onto semiconductor surfaces. One of those methods was suggested by Yamada *et al.* in 2005 [39]. They converted the α -diketone precursor into pentacene through photolysis. In order to produce only pentacene, the photolysis process must be carried out in certain condition, with the absence of oxygen. If oxygen exists, pentacene will transform further into 6,13-pentacenequinone (PQ). The photolysis reaction of α -diketone can be seen in Figure 2.11.

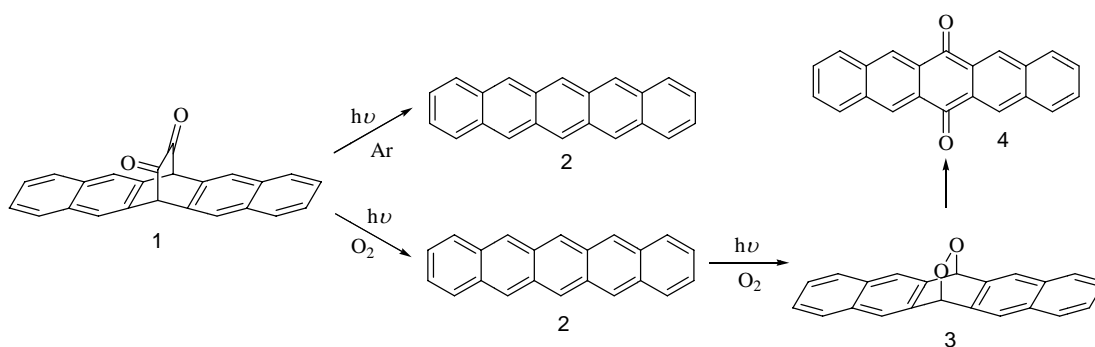


Figure 2.11. Photolysis of α -diketone (1). The absence of oxygen will lead to the pentacene (2) formation. The presence of oxygen will lead to the formation of 6,13-pentacenequinone (4).

Regarding pentacene crystal state, Campbell and co-workers reported the first crystal and molecular structure of pentacene in 1961 [40]. Their study allowed researchers to accurately determine the molecular dimensions of pentacene molecule for the first time. Its length is approximately at 14 Å and the C-C bond lengths range from 1.381–1.464 Å. Pentacene molecular packing is shown in Figure 2.12. The monolayers are characterized by d -spacings of 14.1, 14.5, or 15.0 Å depending on the method of crystallization adopted. Later on, Mattheus and co-workers reported in their works [33, 41] that the pentacene single-crystals commonly adopt the 14.1 Å structure. Figure 2.13 shows an image of pentacene single-crystal.

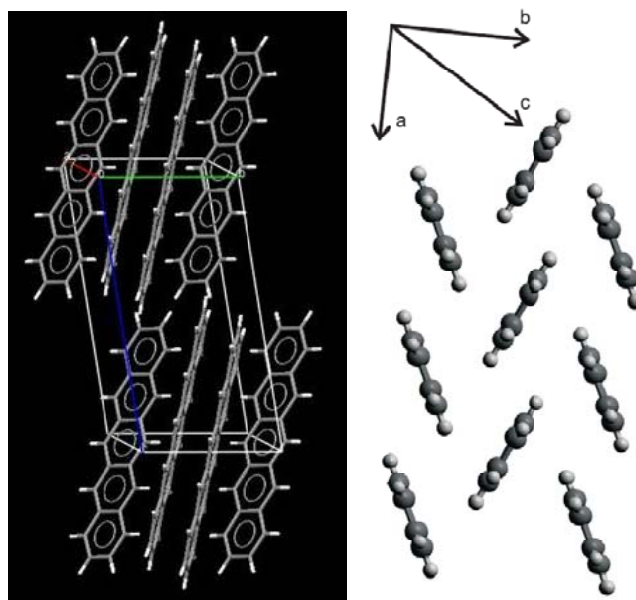


Figure 2.12. Crystal structure of pentacene single crystal. Left panel: view along the [100] axis, the molecules are aligned in parallel along the a (red) and b (green) crystal axis of the unit cell, forming molecular monolayers in the a - b plane. Right panel: the herringbone structure within the layer, view along the long axis of the molecules [28].

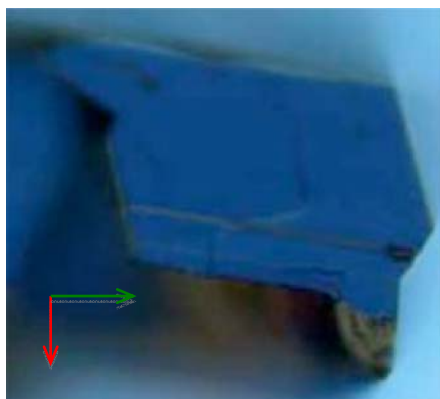


Figure 2.13. Pentacene single-crystal image. The a and b axis indicated by red and green arrow respectively. This image was reproduced from [42].

Pentacene possesses 22 p_z orbitals, each contributing one electron. Its frontier orbitals HOMO and LUMO show a strong contribution from the carbon $2p_z$ orbitals, as shown in Figure 2.14. The $2p_z$ orbitals are the orbital that form the π -bonding and also hold an important role in electron delocalization of polyconjugated organic material (the Peierls distortion, see Section 2.1.2). Thus, the $2p_z$ orbitals will have a strong contribution to the alternation between delocalization state and bond-alternation state (the Peierls distortion) in pentacene, which will influence the molecular conductivity of pentacene. The strong contribution of $2p_z$ orbitals in pentacene's HOMO and LUMO is the molecular reason of pentacene's semiconductivity.

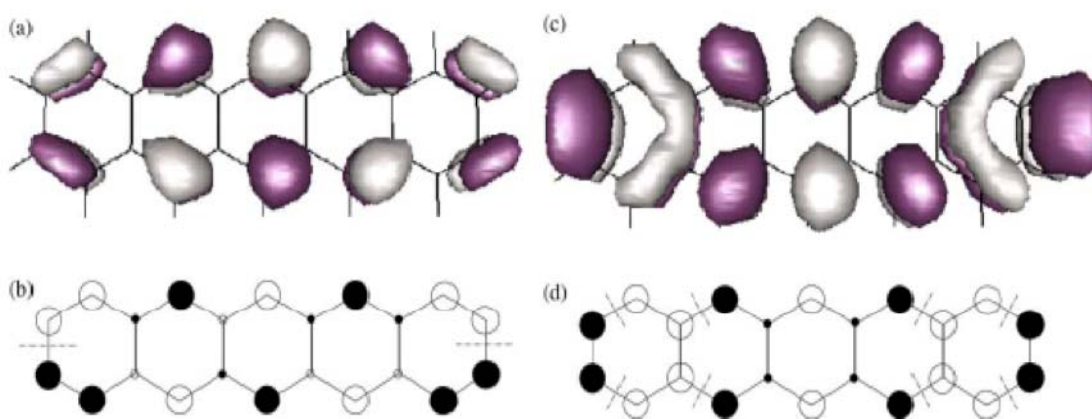


Figure 2.14. Single particle wavefunctions of isolated pentacene molecule. Violet colors and black dots represent positive sign while white colors and white dots represent negative sign. HOMO shows by (a) and (b), LUMO shows by (c) and (d). Reproduced from [43].

2.2.1 Crystal growth of pentacene

Pentacene molecular crystals are formed by weak van der Waals interaction between the molecules. The molecular packing that formed will determine the properties of pentacene crystals, including the electrical properties.

The pentacene single-crystals were grown by physical vapor transport method in a horizontal glass tube under argon stream. Ultrapure argon (without hydrogen) is used in order to prevent the formation of 6,13-dihydropentacene as an impurity in the crystals. 6,13-dihydropentacene can be formed via hydrogenation of the middle ring acene, in position C-6 and C-13, which are the most reactive positions [32].

The starting material is purified pentacene. The pentacene starting material was purified by vacuum sublimation under a temperature gradient. The aim of purification is to eliminate 6,13-pentacenequinone from the starting material [32].

The purified pentacene is placed in a glass or quartz tube, heated by resistive heater coils around the tube to its sublimation temperature, and carried down a temperature gradient by a stream of argon. The pentacene resublimates in the cooler zone of the furnace to form crystals. Heavy impurities with a vapor pressure lower than that of the pure organic compound remain at the position of the source material (downstream). Light impurities with a vapor pressure higher than that of the pure organic compound condense at a lower temperature, *i.e.* at a different position from where the crystals grow (see Figure 2.15). During crystal growth, a proportionally large fraction of the impurities is deposited on the surface, which then again can sublime and crystallize further along the crystallization tube. The single-crystals are collected from glass or quartz sleeves. The illustration of physical vapor transport set-up is shown in Figure 2.15.

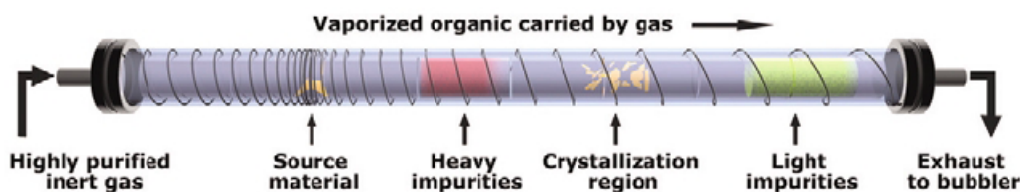


Figure 2.15. Physical vapor transport diagram. Pentacene single-crystals were made by this technique with argon as the inert gas. Image was taken from [18].

In this work, the whole crystal growth process was done by Solid State Chemistry of the Materials Science Centre at the University of Groningen since the pentacene single-crystals that were used in this research was supplied by them.

2.2.2 Pentacene single-crystal

As mentioned earlier in this report, the pentacene single-crystal system is commonly selected in order to study the intrinsic properties of pentacene. By using the single-crystal system, grain boundaries are eliminated. Besides, in order to explore the intrinsic properties of organic materials and the physical limitations on the performance of organic FET, devices based on single-crystals of organic semiconductors are needed, similar to the single-crystal structures of inorganic electronics.

However, other factors also play an equally important role in electrical characterization. The surface of the pentacene single-crystal holds an important role in the fabrication of pentacene single-crystal field-effect transistor, mainly in the contact between pentacene and electrodes since surface impurities can increase the resistance for charge injection from the electrode through the impurities into the pentacene. It also influences the pentacene/dielectric interface, as in a FET conducting channel will be formed in there. Thus, the cleanliness of the pentacene surface will influence the performance of the single-crystal field-effect transistor.

One of the aims of this work has a correlation with the presence of impurities on pentacene surface, the oxidation product of pentacene, 6,13-pentacenequinone. The presence of PQ in the crystals is caused either by oxidation after the crystal has been grown or is caused by co-deposition of PQ from impure pentacene source when the crystal growth was conducted. The formation of PQ via photo-oxidation of pentacene has been explained in the previous section (see Figure 2.11).

2.2.3 Pentacenequinone on pentacene single-crystal surface

The main impurity in commercial pentacene powder and carefully grown pentacene single-crystals is 6,13-pentacenequinone (PQ), as mentioned in several publications [13, 32, 44-48]. The PQ impurities were concentrated in the surface of the pentacene single-crystal due to the inhomogeneous distribution of PQ during the pentacene single-crystal growth [44, 48].

Another mechanism to explain the presence of PQ on the pentacene surface is the oxidation of pentacene molecular layers that are exposed to light and oxygen from air after the crystals are grown. Pentacene molecules are oxidized, forming a PQ layer. Bulk PQ crystallizes in 1.779 nm thick layers [44], consisting of two alternating PQ monolayers. PQ monolayers (0.89 nm) are thinner than pentacene monolayers (1.41 nm) [44]. From these step height data, crystal model of pentacene and PQ was made as shown in Figure 2.16. The crystal model shows the presence of possible steps height that will be formed by combining the pentacene and PQ layers.

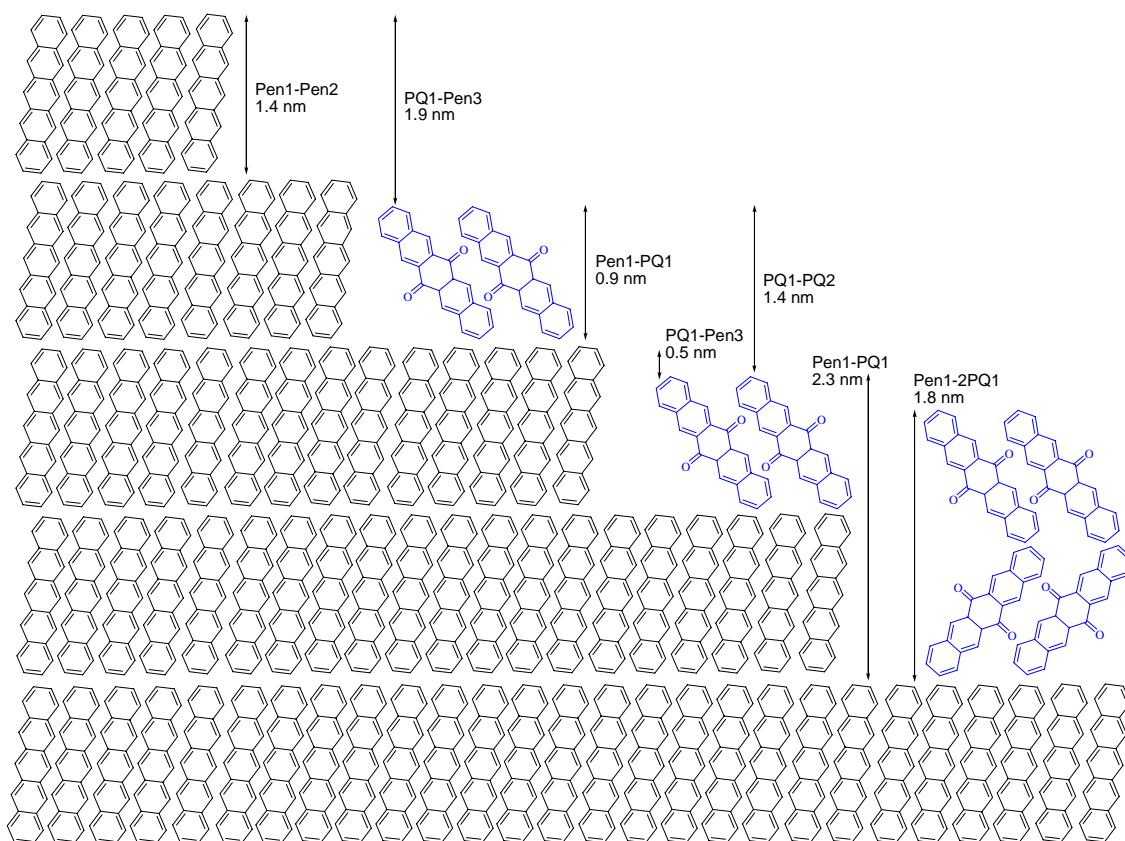


Figure 2.16. Model of pentacene and pentacenequinone packing system, viewed perpendicular from c crystal direction [44, 49].

The AFM study of pentacene single-crystal surface by Peter de Veen [50] indicates that the PQ molecules form a typical molecular flat terraces with various height. The height of the terraces depends on the molecular layers. Step height statistic of pentacene single-crystal surface from the AFM (Figure 2.17) shows that the PQ monolayer on the surface of pentacene has a height of 0.9 nm, while the PQ double-layers in the pentacene surface has a height of 1.8 nm. It also shows pentacene step at the surface of pentacene single-crystal (1.4 nm), which match with the work of Jurchescu and co-workers [44].

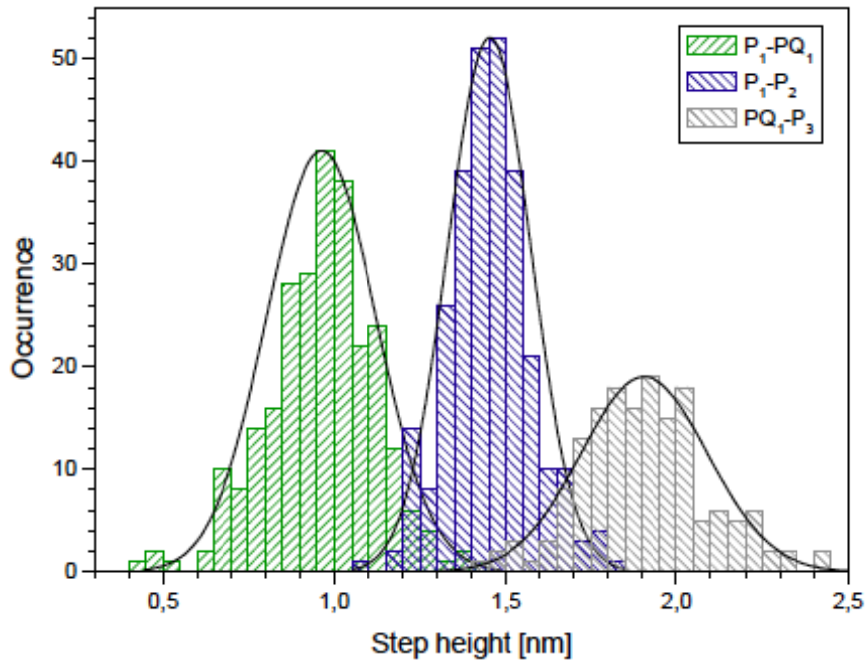


Figure 2.17. Statistical AFM step height data of pentacene single-crystal surface. Green, blue, and grey colors corresponds to 6,13-pentacenequinone (PQ) monolayers, pentacene bilayers (P), and 6,13-pentacenequinone (PQ) bilayers, respectively [49].

2.3 Space-charge-limited current

Charge transport in organic conductors is often limited by the emergence of space charges. To evaluate the conduction in the space-charge-limited current (SCLC) regime, two limiting geometries can be used. The Mott-Gurney theory describes the current-voltage characteristics for sandwich-type contact geometries [51]. In this theory, the electric field and the space charge are confined to the channel. The Mott-Gurney law for sandwich-type structure gives an expression as shown in Equation 2.4.

$$J = \frac{9\Theta\mu\varepsilon_0\varepsilon_r}{8} \left(\frac{V^2}{L^3} \right) \quad \text{Equation 2.4}$$

In Equation 2.4, J is the current density for the applied voltage V , Θ is the trapping factor, L is the distance between electrodes, ε_r is the relative dielectric constant of the materials, ε_0 is the vacuum permittivity constant, and μ is the charge carrier mobility.

In Mott-Gurney theory, several considerations were taken: (1) the current flow is a one-dimensional unipolar flow (charge carriers are injected from the contact placed at position $x = 0$ and collected at the contact at $x = L$); (2) the contacts are Ohmic; (3) the mobility of free charge carriers is inde-

pendent of the magnitude of the applied electric field; (4) the injecting contact is an infinite source of charge carriers; (5) the traps are homogeneously distributed in space and all correspond to one discrete energy level; and (6) the diffusion of charge carriers inside the crystal is neglected [22].

Another theory was developed by Geurst [52]. Geurst analyzed SCLCs in thin semiconductor layers for a gap-type geometry theoretically. In this theory, the thickness of the film is negligible with respect to the separation between the contacts. For this geometry, longitudinal component of the electric field is responsible for the charge transport and the transversal component, perpendicular to the conduction channel, is determined by the magnitude of the space charge. The Geurst gap-type structure reveals a relation as seen in Equation 2.5, I is the current for the applied voltage V , L is the distance between electrodes, ϵ_r is the relative dielectric constant of the materials, ϵ_0 is the vacuum permittivity constant, and μ is the charge carrier mobility.

$$I = \frac{2\mu\epsilon_0\epsilon_r}{\pi} \left(\frac{V^2}{L^2} \right) \quad \text{Equation 2.5}$$

In his report, Zuleeg and Knoll [52] introduce the width of the electrodes W into the Equation 2.4 and 2.5. It improves the approximation of Geurst's infinite contact length. By introducing W , Equation 2.5 becomes Equation 2.6.

$$I = \frac{2\mu\epsilon_0\epsilon_r W}{\pi} \left(\frac{V^2}{L^2} \right) \quad \text{Equation 2.6}$$

An illustration of Mott-Gurney sandwich-type structure and Geurst gap-type structure is shown in Figure 2.18. The gap-type structure is the electrode geometry that was used in this work.

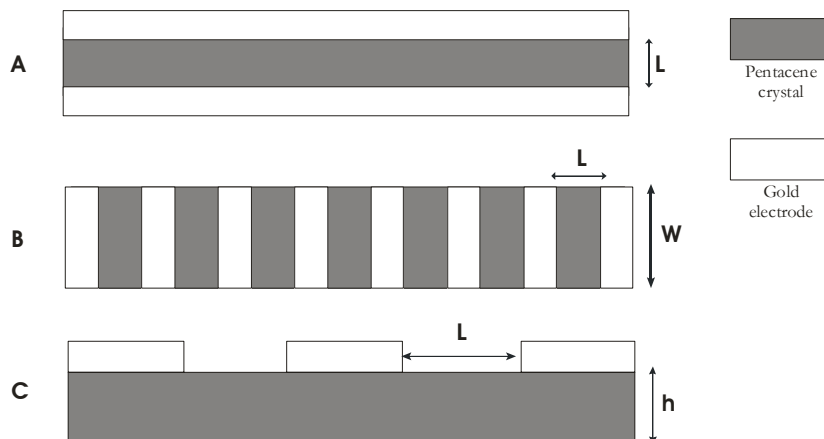


Figure 2.18. Electrode geometries: (A) sandwich-type structure, side view; (B) gap-type structure, top view; and (C) gap-type structure, side view.

Theoretical I - V characteristic for a material with a single trap level in a double-log scale is shown in Figure 2.19. It shows the crossover from the Ohmic region ($I_{\Omega} \sim V$) to the SCLC with the presence of shallow trapping region ($I_{SCLC} \sim V^2$), and, with a further voltage increase, to trap-free (TF) region and SCLC without trapping region ($I_{SCLC,TF} \sim V^2$).

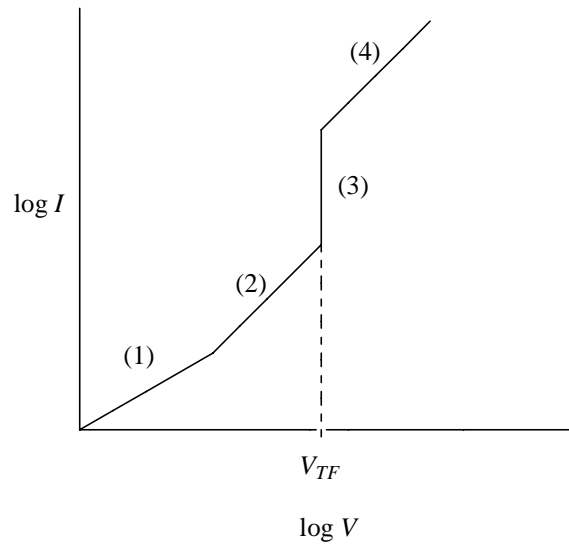


Figure 2.19. Schematic of current vs voltage characteristic for a material with a single trap level: (1) Ohmic region supported by thermal generation, (2) SCLC region with the presence of shallow trapping, (3) trap-filled limit, (4) SCLC region with the absence of trapping. Adapted from [22].

From the threshold voltage of the TF regime, V_{TF} , the density of deep traps, N_t^d , can be estimated [22]:

$$N_t^d = \frac{\epsilon\epsilon_r V_{TF}}{eL^2} \quad \text{Equation 2.7}$$

An assumption-free estimate of the trap density can be made only if a well-defined crossover between SCLC and TF regimes is observed. For this reason, the method can be applied only to sufficiently pure crystals.

The estimate of N_t^d is based on the assumption that the deep traps are uniformly distributed throughout the entire crystal bulk. However, it is likely that the trap density is greater near the metal/organic interface because of the surface damage during the contact preparation. A small amount of traps located close to the surface can have a large effect on current flow: the charges trapped near the surface strongly affect the electric field in the bulk of the crystal, which determines the cur-

rent flow in the TF regime. For this reason, the value of N_t^d may be considered as an upper limit of the actual density of traps in the bulk [53].

In the TF regime, the mobility can be estimated from the Mott-Gurney law for trap-free regime [22]:

$$J_{TF} = \frac{9\mu\epsilon_0\epsilon_r}{8} \left(\frac{V^2}{L^3} \right) \quad \text{Equation 2.8}$$

Even when the TF limit is not experimentally accessible, the same formula can be used to extract a lower limit, μ_{min} for the intrinsic mobility, at least in materials in which one type of carriers (holes or electrons) is responsible for charge transport [53]. We can say that the μ_{min} is equal to $\mathcal{O}\mu$.

In 2003, Mattheus and co-workers reported the current-voltage characteristic of single crystalline pentacene (see Figure 2.20). From their analysis, they found out that the hole mobility and trap density for their pentacene single-crystal are $0.2 \text{ cm}^2 \text{ V}^{-1} \text{ s}^{-1}$ and $2 \times 10^{13} \text{ cm}^{-3}$, respectively [33]. Several researchers also have reported the SCLC measurements on single-crystal systems, such as tetracene [53] and rubrene [54] single-crystal systems.

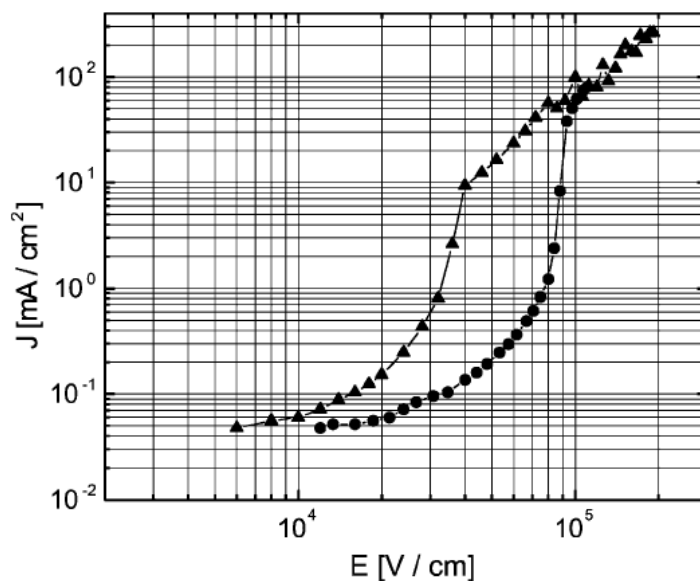


Figure 2.20. Current-voltage characteristic of pentacene single-crystal: (▲) gap 50 μm ; (●) gap 75 μm . Reproduced from [33].

Chapter 3 Experimental

3.1 Equipments

3.1.1 Nanomanipulator system

SEM images were taken by JEOL 6490 scanning electron microscope (SEM). The SEM system is part of a nanomanipulator system consists of Keithley 4200 source measure unit and the Zyvex s100 Nanoprober. The Nanomanipulator system is designed to conduct electrical characterization (Keithley 4200 source measure unit) and mechanical manipulation (Zyvex s100 Nanoprober) in nano-scale. The ultimate pressure in SEM vacuum chamber is 0.1 mPa (1×10^{-6} mbar).

Carbon fibers were used as the tip of the nanomanipulator probes. The carbon fibers were coated by gold to make sure that the electrical current flow from one probe to another flawlessly. Figure 3.1 shows the image of the gold-coated carbon tips.

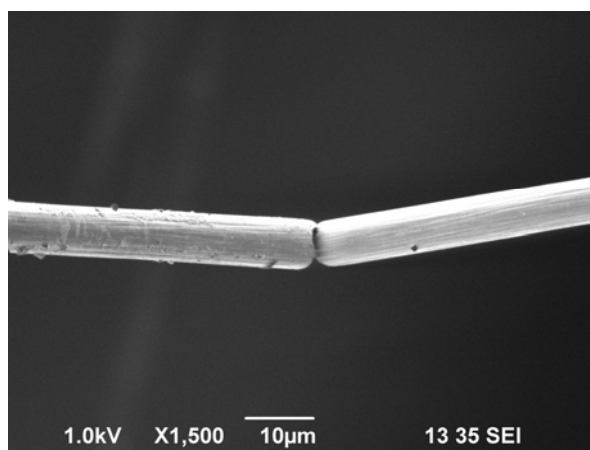


Figure 3.1. SEM image of gold-coated carbon fibers that were used as the probes.

3.1.2 Heater set-up

To do the *in-situ* heating treatment, a special heating system was made. The heating system was using a free-standing set-up with Heraeus HA 421 as the heater. The free-standing set-up was used to make sure the heat from the heater only went to the sample.

3.1.3 Pulsed laser deposition system

The Pulsed laser deposition system consisted of a vacuum chamber with optical window, a target of the deposition material, a sample holder with heater, and lens system to direct the pulsed laser radiation from a LPX2000 KrF excimer laser (248 nm 25 ns) to the target. Stencils were used as shadow mask to deposit Au-contacts in order to fabricate the space-charge-limited current devices.

3.2 Pentacene single-crystal surface characterization

3.2.1 Sample preparation

To make the sample, pentacene single-crystal was glued carefully on a silicon substrate by silver paste to secure the crystal in place.

3.2.2 SEM characterization

SEM was used to observe and investigate the surface of pentacene single-crystals. As mentioned earlier, investigation of PQ impurities on the pentacene single-crystals surface is one of the aims in this research. Since pentacene surface layer is our only concern, low acceleration voltages, 0.3 and 0.5 kV, were used in this research to observe only the surface layers instead of the deeper layers in the pentacene single-crystal.

3.2.3 *In-situ* heat treatment

The pentacene single-crystal surface can be cleaned from PQ impurities through heating process since the sublimation behavior of pentacene and PQ are different (see Figure 3.2). However, the difference is very small, so the heating process must be carried out with extreme cautious. Figure 3.2 shows the sublimation rate of pentacene and PQ bulk powder in vacuum. The small difference in sublimation behavior and the fact that this behavior is for bulk powder are assumed applicable in our system.

Gerard van Bommel has done the cleaning process and reported the result in his thesis [49]. He cleaned the pentacene single-crystal surface and observed the sublimation of PQ simultaneously through the *in-situ* heat treatment using a small heater. The observation was done by using SEM system. The *in-situ* heat treatment in this work was done according to van Bommel's work.

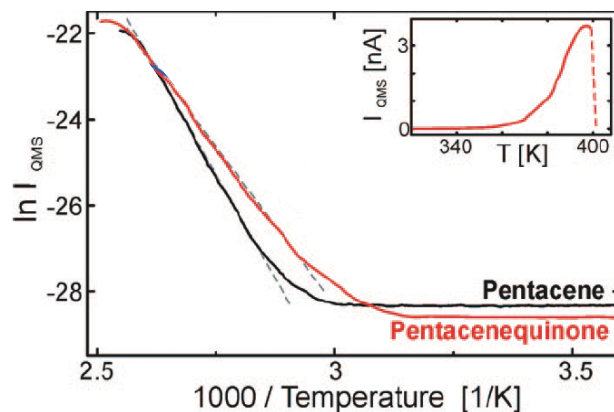


Figure 3.2. Sublimation rate of pentacene and PQ in vacuum as a function of temperature (thermal desorption). Inset shows a typical thermal desorption spectrum for PQ. Adapted from [55].

3.3 Electrical characterization of pentacene single-crystal device

The other aim of this work is to extract charge carrier mobility value of pentacene using the space-charge-limited current (SCLC) method. The SCLC devices that we designed have a gap-type structure. The relation between electrical current (I) with voltage (V) in the gap-type structure is described by Equation 2.5 and 2.6.

As mentioned before, gold was used as the electrodes. The planar Au-contacts were deposited on pentacene single-crystal surface by using PLD technique. The SCLC device can be seen in Figure 3.3. The pentacene single-crystal that was used in the SCLC device still contains PQ layer on its surface (untreated).

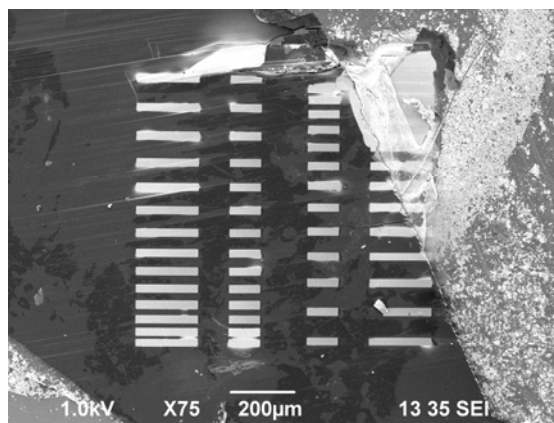


Figure 3.3. SEM image of the SCLC device. The Au-electrodes were arranged in gap-type geometry. The PQ also can be observed in the surface of pentacene.

The I - V measurements were done by using Keithley 4200 source measure unit. Probes were placed in the electrodes, as shown in Figure 3.4. The two-point measurement was used with the voltage sweeping from 0 to 200 V.

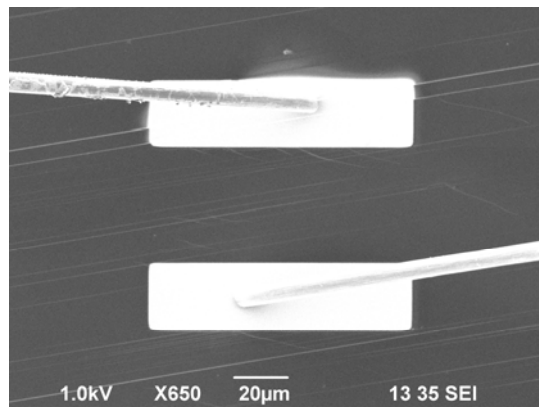


Figure 3.4. Probes landed at the Au-contacts. The shadows below the probes indicate the probes have made contact with the electrodes.

Chapter 4 Results and Discussion

4.1 Pentacene single crystal surface

4.1.1 SEM characterization

Figure 4.1 shows the scanning electron microscope image of pentacene single-crystal surface. As seen on the image, thin layer of PQ is observable on the surface of pentacene single-crystal. The PQ layers are only observable by SEM in low acceleration voltages (0.3 kV and 0.5 kV) as mentioned before in the experimental section. The light grey patches in the crystal surface show the PQ terrace steps. In his work, van Bommel has checked the area with light-grey patches by AFM [49]. He proved that the light grey patches are PQ layers.

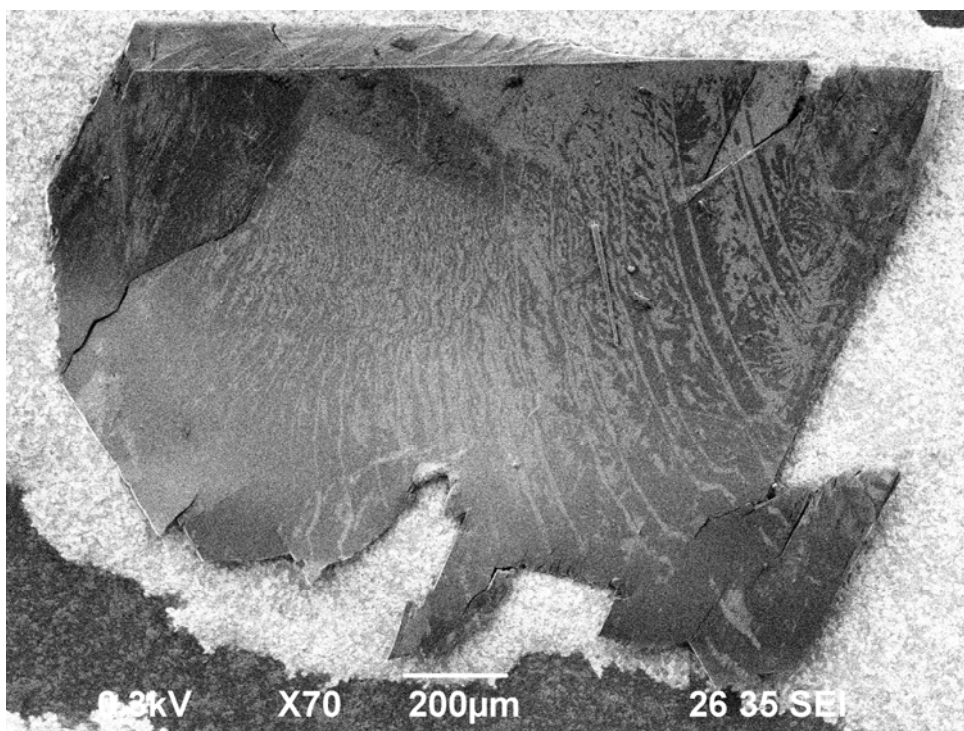


Figure 4.1. SEM image of pentacene single-crystal surface at low acceleration voltage (0.3 kV). The light grey irregular shaped patches are the 6,13-pentacenequinone layers.

4.1.2 *In-situ* heat treatment

The heat treatment was conducted inside the electron microscope vacuum chamber by using a heater with custom configuration, as explained before in Section 3.1.2. The investigation of selective sublimation of PQ is conducted by taking a sequence of SEM images during the heating process. Three temperatures have been investigated (82°, 91°, and 100°C), in order to get a good temperature point to observe the selective sublimation of PQ layer. In this process, the investigation of sublimation temperature is very important since we knew that pentacene and PQ have a small difference in sublimation point. Through the investigation, we found that 82°C is the best temperature to observe the sublimation of PQ. This result is supported by the previous work of van Bommel [49]. During the investigation, it also has been found that by increasing temperature to 91° and 100°C not only the PQ layer that will sublime, the pentacene layer will also sublime. Figure 4.2 shows a sequence of pentacene sublimation. The sublimation of pentacene is obviously unwanted.

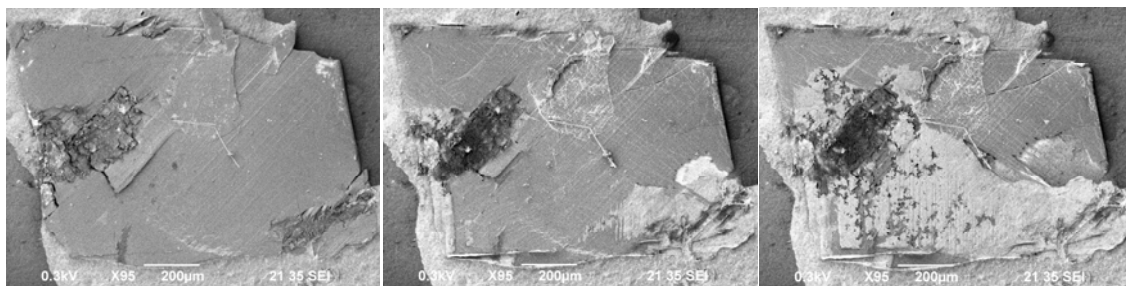


Figure 4.2. SEM images of overheated pentacene single-crystal. Times increased from left to right.

Figure 4.3 shows the best heat treatment result for one of our samples. For this sample, the approximate time that was needed to achieve a complete sublimation of PQ surface layer was 80 minutes.

There are several issues regarding the observation of *in-situ* heat treatment by SEM system that worth to be mentioned:

- (1) The details of pentacene surface when the heater was on and off is different. Figure 4.3(A) and (G) show the pentacene single-crystal condition before the heat treatment was started. The difference is only in the heater condition: in Figure 4.3(A) heater was on, while in Figure 4.3(G) heater was off. If we compare the two images carefully, we will find several regions that were light grey in Figure 4.3(G) turned darker in Figure 4.3(A) and *vice versa*, the regions that were darker in Figure 4.3(G) turned lighter in Figure 4.3(A). Although, the reason behind this phenomenon is still unclear, there is a high chance that it was caused by the heat conduction from the heater to the crystal since the SEM images were back to normal when the heater was turned off. The heat conduction in the crystal surface interferes the

scanning process in SEM system. This phenomenon was also observed in other pentacene single-crystal samples,

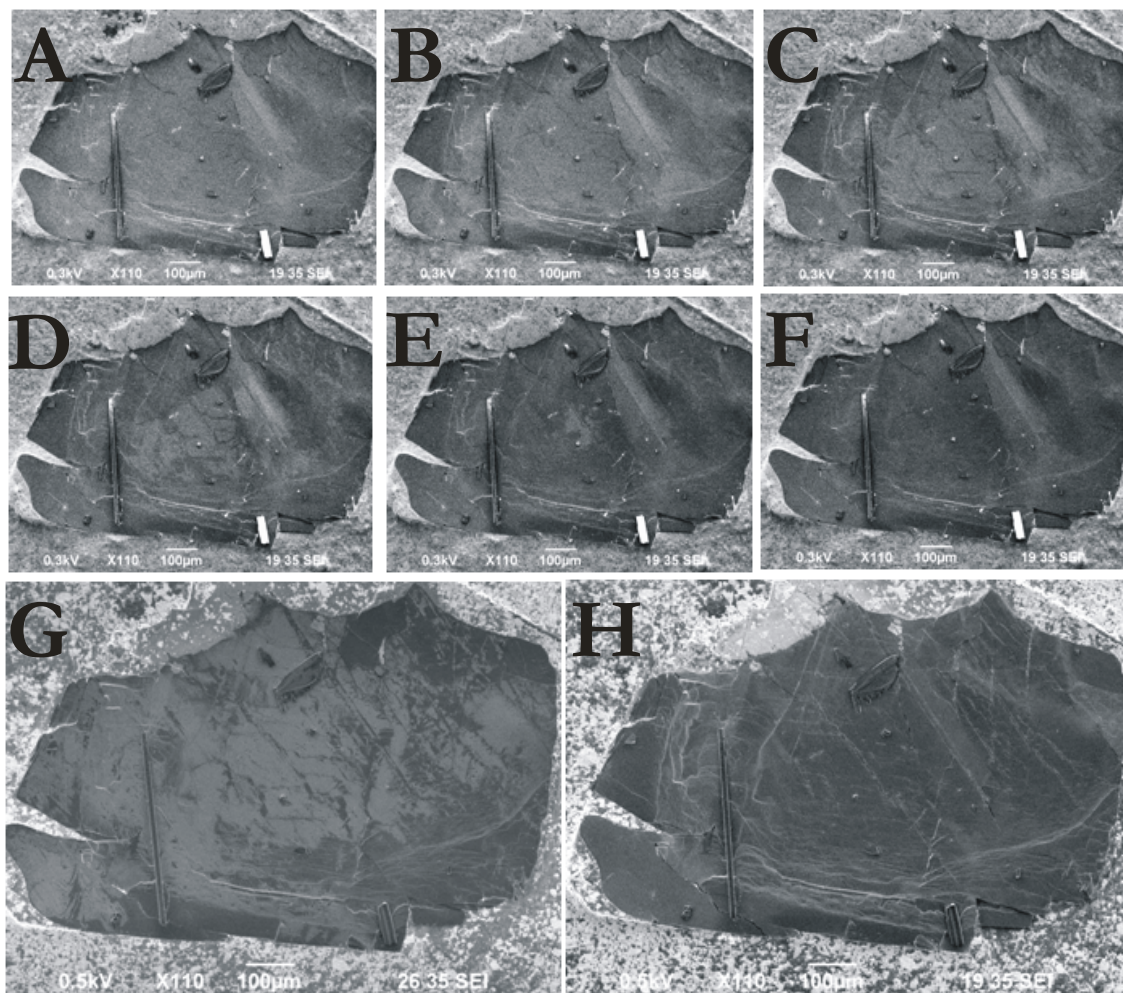


Figure 4.3. SEM images of pentacene single-crystal sample before (G) and after (H) heat-treatment (heater was off when these images were taken). Image A to F show a sequence of sublimation process that happened inside the vacuum chamber. The sublimation of PQ started from the edge of the crystal and ended at the center.

- (2) By using SEM system, we cannot capture images too often since if we do it carbon layer will be formed quickly on the pentacene surface. Thus, it will make more difficult to observe the sublimation of PQ,
- (3) It is difficult to measure exact amount of PQ molecules that were sublimed from SEM images in order to do quantitative analysis. Although Gerard van Bommel proposed a mapping technique to calculate the exact amount of PQ molecules [49], it seems that technique has a weakness: it needs an image with high contrast. In the SEM images, the contrast value between the light grey (PQ) and dark grey (pentacene) is too low. Even after the image

processing, the contrast is not high enough to enable a good mapping of pentacene and PQ layer. Therefore, this technique is not good enough to extract accurate data from SEM images with vague PQ patches on the pentacene single-crystal surface.

Despite its weaknesses, the *in-situ* heat treatment with SEM monitoring can be used to clean pentacene single-crystal surface to get a good pentacene/electrode and pentacene/dielectric interfaces in FET devices. However, it is only applicable for qualitative analysis.

4.2 Electrical characterization of pentacene single-crystal device

The SCLC measurements were conducted inside the electron microscope vacuum chamber, which provided a vacuum of 0.1 mPa (1×10^{-6} mbar), dark, and room temperature conditions. The measurements were done by varying the distance between electrodes (L). The L values were ranged from 10 to 65 μm , while the width of the electrodes (W) was 100 μm .

Curve fitting was used to determine whether the measurement results have Ohmic and SCLC regimes or not. The curve fitting was done by fitting the measurement data with $y = ax^b$ function. Not all of our data exhibit the I - V characteristic as shown in Figure 2.19, only 8 of 75 that show Ohmic-SCLC crossover in the I - V curve. The other measurement results have no Ohmic and SCLC regime since their current-voltage relation at low voltages shows no Ohmic current and full of noise, while at higher voltages shows no square law dependence of the current with the applied voltage (SCLC regime). One of the data that shows Ohmic-SCLC crossover in its I - V curve is shown in Figure 4.5.

During the measurement, we observed that at some point, when the voltages were high enough (above 120 V), the pentacene surface will blow-up, forming holes as seen in Figure 4.4.

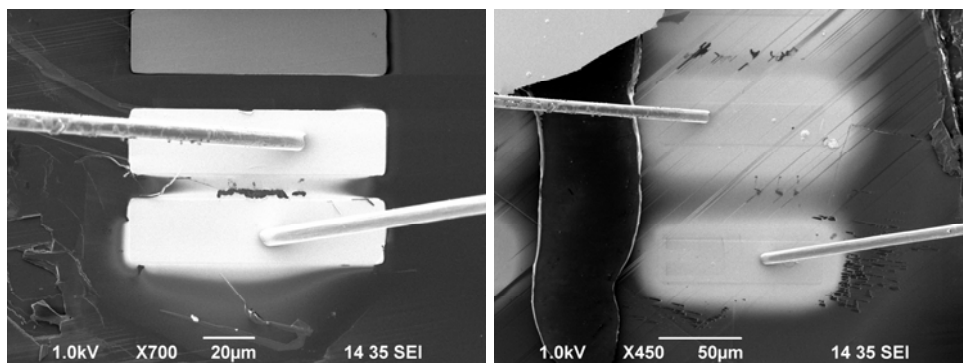


Figure 4.4. Holes were formed on pentacene surface because of the use of high voltage.

When this phenomenon occurs, the charge transport between electrodes will be disturbed. Thus, the measurement results will be inaccurate and will show a lot of noise. The measurement results also show no Ohmic and SCLC regime when we plot the I - V curve of those data. This blow-up phenomenon only happened when the measurements were conducted in two electrodes with short distance.

Figure 4.5 shows the I - V curve of pentacene single-crystal measured in a - b plane (in double-log scale). At low voltages, the current is Ohmic. At higher voltages, the square law dependence of the current with the applied voltage is observed, corresponding to the SCLC regime. Small deviation from the linear and quadratic regimes can be attributed to the non-linear contribution of Schottky barriers formed at the gold/pentacene interface [56]. We did not observe trap-free limit in all of our measurement results.

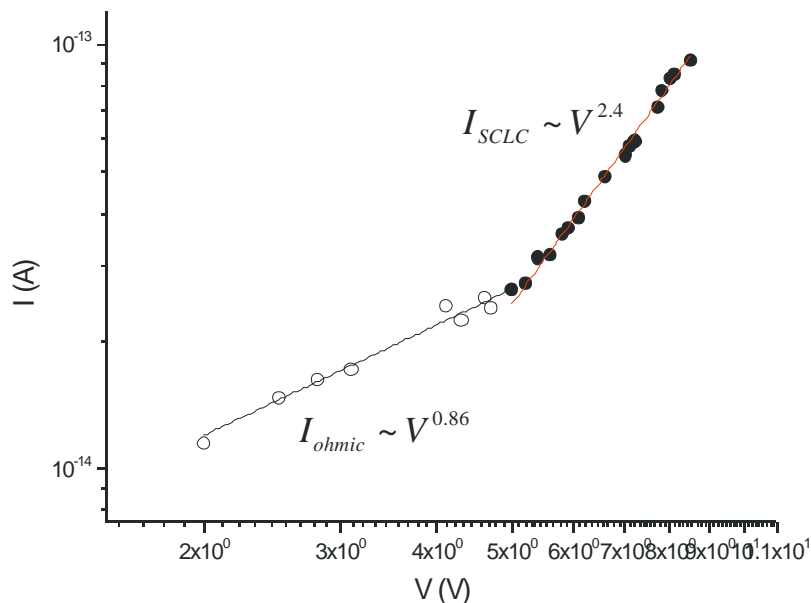


Figure 4.5. Current I vs applied voltage V (in double-log scale) for pentacene single-crystal at room temperature, in vacuum and dark. Ohmic regime is shown by black line while the SCLC regime is shown by red line.

Equation 2.6 was used to calculate the charge carrier mobility. The relative dielectric constant of pentacene is assumed to be 3 [57]. Since the trap-free regime was not experimentally accessible in all of our measurement results, we are only able to calculate $\Theta\mu$. The $\Theta\mu$ values are shown in Table 4.1. From 8 measurement data, only 5 data were used to calculate the $\Theta\mu$. The other 3 data were obtained from different SCLC device. Thus, we cannot compare them with our other 5 data.

Table 4.1. The lower limit intrinsic mobility ($\Theta\mu$) values with their corresponding distance between electrodes (L).

No	L (μm)	$\Theta\mu$ ($\text{cm}^2 \text{V}^{-1} \text{s}^{-1}$)
1	10	2.356
2	25	1.985×10^{-6}
3	30	1.206×10^{-6}
4	35	2.973×10^{-6}
5	37.5	3.362×10^{-4}

As shown in Table 4.1, the $\Theta\mu$ values that we obtained from the calculation are relatively small, except for number 1. Result number 1 shows the highest $\Theta\mu$ value because gold layer was also deposited in between two electrodes. Thus, it will enhance the current flow between two electrodes, which is unwanted. The electrodes condition for each measurement is shown in Figure 4.6. By plotting data in Table 4.1, we can see that there is no particular trend in these data (see Figure 4.7).

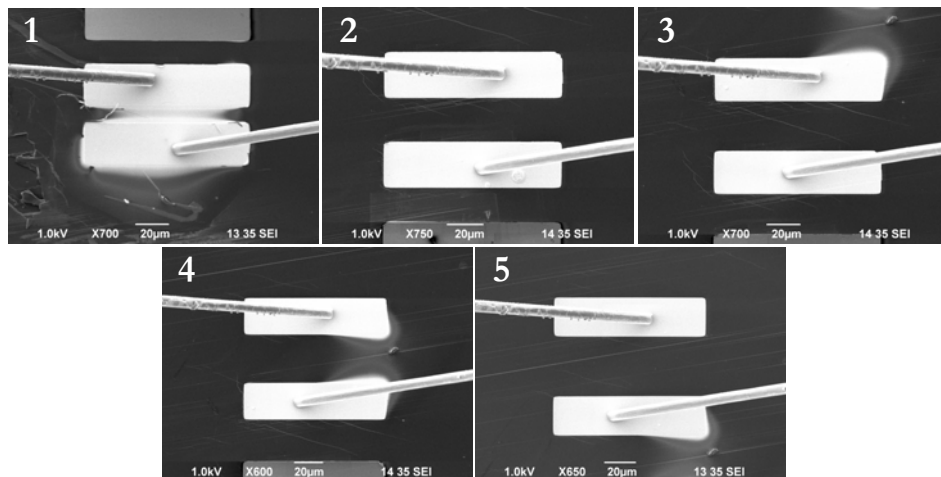


Figure 4.6. Electrodes condition during the I - V measurement. Each number corresponds with the result number in Table 4.1.

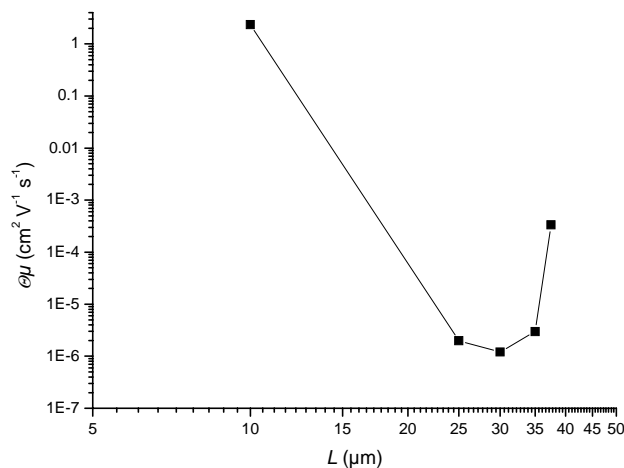


Figure 4.7. The relation between lower limit intrinsic mobility with the electrode separation. No particular trend observed in this curve.

Regarding the trap-filling limit regime, Mattheus has reported the relation between vacuum condition during the I - V measurement with the observation of trap-filling limit regime [57]. She measured the I - V characteristic in two different conditions: in air and in a high vacuum pressure condition (2×10^{-7} mbar). The trap-filling limit was not reached in the measurements in air, while it was reached in high vacuum pressure condition. However, the reproducibility of the measurements was rather low. After two measurements, she had to wait for at least 12 hours before the trap-filling regime could be observed again. If we compare the vacuum pressure condition that we used in our measurements (1×10^{-6} mbar) with the one that Mattheus used, the vacuum pressure condition that we used is a bit lower than the vacuum pressure condition that Mattheus used (2×10^{-7} mbar). Although the difference is rather small, it is worth to try increasing the vacuum pressure that we use in order to observe the trap-filling limit regime.

Several publications have reported the hole mobility for pentacene single-crystal, most notably [18, 33, 34, 56]. In those report, the values of hole mobility are ranging from 0.2 to 2.2 $\text{cm}^2 \text{V}^{-1} \text{s}^{-1}$. These values are far higher than what we obtained. Apart from the fact that the pentacene single-crystal that we used to fabricate the SCLC device still contains PQ layer on its surface, the reasons lie on the electrode/probe interfaces and the material that we used to make the probe.

The electrode/probe interface and the probe material in [33, 56] are different compared to what we used. Jurchescu and co-workers were using silver epoxy as the electrodes [56], while Mattheus and co-workers were using 10 nm titanium and 40 nm gold as the electrodes [33]. Both Jurchescu *et al.* and Mattheus *et al.* were using platinum wires that were connected to the electrodes with silver epoxy to do the I - V measurement [33, 56]. We used gold-coated carbon fiber to measure the I - V

measurement and to do the measurement we only put the carbon tips to the electrodes without gluing them with something, *e.g.* silver epoxy. There is a possibility that we only had minimum contact between the probes and electrodes and as a result the electric current from the probe to the gold electrode was quite small. Thus, the charge carrier injection from gold electrode to the pentacene will also be small, which lead to the low charge carrier mobility.

4.3 Discussion

The *in-situ* heat treatment aim is to remove the PQ layer from pentacene single-crystal surface through sublimation. Here, we used SEM to monitor the sublimation of PQ layer. However, there are some issues regarding the SEM monitoring method, as mentioned before. From this research, we know that SEM only can be used to monitor the sublimation for qualitative analysis purpose. In order to do quantitative analysis, we need to obtain data from SEM images, which is quite impractical and not good enough in term of accuracy. Therefore, in order to get more information regarding the sublimation process of PQ (quantitative analysis), we need more reliable monitoring system.

Here, we also fabricate pentacene single-crystal based SCLC device to study the intrinsic electronic properties of pentacene through the I - V measurement. However, from 75 measurements we only found 8 measurements that exhibit Ohmic and SCLC regime in the I - V curve. The $\Theta\mu$ values that we got from calculation were also relatively low compared to the literature, except for the data number 1 since there was a gold layer deposited in between the two electrodes (which is unwanted). The reason for small $\Theta\mu$ values that we got and the measurement error (in our case is high noise) are because of the minimum contact between carbon tips (probes) and electrodes, and the carbon tips itself. Although the carbon fibers were coated by gold, it seems the coating does not help much for the electrical conduction from the source measure unit to the electrodes. Jurchescu *et al.* and Mattheus *et al.* were using platinum wires to connect the electrode with the source measure unit, which are much better electrical conductor than carbon fibers. They also were using silver epoxy to connect the platinum wires to the electrodes. Thus, the contact between wires and electrodes was maximum. From Mattheus report [57], we also conclude that the vacuum pressure also needs to be increased in order to observe the trap-filling limit regime.

Chapter 5 Conclusion and Suggestions

5.1 Conclusion

The *in-situ* heat treatment is can be used to remove the PQ layer from pentacene single-crystal surface. However, the current monitoring system by SEM is only useful to do the qualitative analysis of PQ sublimation and it also has several drawbacks. A temperature of 82°C is the best point to remove the PQ layer from pentacene single-crystal surface.

The lower limit intrinsic mobility ($\theta\mu$) values are successfully extracted from the I - V measurement. We are only able to obtain $\theta\mu$ values since the trap-filling limit regime was not observed in our measurements. The $\theta\mu$ values from our measurement are relatively low compared to the literature. There are several issues that can be addressed as the reason behind the low value of $\theta\mu$ that we have got, apart from the fact that the pentacene single-crystal that was used to fabricate the SCLC device is still contains PQ. The reasons are related with the material that was used to connect the electrodes with the source measure unit (probes material) and the contact between the probes with the electrodes.

5.2 Suggestions

It is highly recommended to replace the current *in-situ* heat treatment monitoring system (the SEM system) with another system that will enable accurate and precise monitoring of PQ layer on the pentacene single-crystal surface. Thus, a quantitative analysis of PQ sublimation can be done with the help of this new monitoring system. AFM system can be used to replace the SEM system as the monitoring system.

As for the I - V measurement, it is recommended to replace the carbon fiber as the tip of the nano-probe. Although the carbon fibers were coated by gold, it seems the coating did not help much for the electrical conduction from source measure unit to the electrodes. Thus, a better electrical conductor must be used to replace the carbon fibers, *e.g.* platinum. We also need to maximize the contact between probes and electrodes, *e.g.* by gluing them with silver epoxy. Vacuum pressure also needs to be increased in order to observe trap-filling limit regime. More importantly, the investiga-

tion regarding the influence of PQ impurities removal on pentacene single-crystal electrical properties is needed to be conducted.

References

1. Arns, R.G., *The other transistor: early history of the metal-oxide-semiconductor field-effect transistor*. Engineering Science and Education Journal, 1998. **7**(5): p. 233-240.
2. Koezuka, H., A. Tsumura, and T. Ando, *Field-effect transistor with polythiophene thin film*. Synthetic Metals, 1987. **18**: p. 699-704.
3. Tsumura, A., H. Koezuka, and T. Ando, *Polythiophene field-effect transistor: Its characteristics and operation mechanism*. Synthetic Metals, 1988. **25**(1): p. 11-23.
4. Kodak. *OLED Technology - "Enabling the OLED Industry"*. 2009 [cited 2009 September 10th]; Available from: http://www.kodak.com/eknec/PageQuerier.jhtml?pq-path=1473&pq-locale=en_US&requestid=6895.
5. Pogantsch, A., et al., *Tuning the Electroluminescence Color in Polymer Light-Emitting Devices Using the Thiol-Ene Photoreaction*. Advanced Functional Materials, 2005. **15**(3): p. 403-409.
6. Bansal, R., *Coming soon to a Wal-Mart near you*. IEEE Antennas & Propagation Magazine, 2003. **45**(6): p. 105-106.
7. Baude, P.F., et al., *Pentacene based RFID transponder circuitry*, in *Device Research Conference, 2004. 62nd DRC. Conference Digest*. 2004. p. 227-228.
8. Kline, R.J., et al., *Controlling the Field-Effect Mobility of Regioregular Polythiophene by Changing the Molecular Weight*. Advanced Materials, 2003. **15**(18): p. 1489-1567.
9. Huitema, H.E.A., et al., *Plastic transistors in active-matrix displays*. Nature, 2001. **414**: p. 599.
10. Andersson, P., et al., *Active Matrix Displays Based on All-Organic Electrochemical Smart Pixels Printed on Paper*. Advanced Materials, 2002. **14**(20): p. 1460-1464.

11. Reese, C. and Z. Bao, *Organic single crystals: tools for the exploration of charge transport phenomena in organic materials*. Journal of Materials Chemistry, 2006. **16**: p. 329-333.
12. Boer, R.W.I.d., et al., *Organic single-crystal field-effect transistors*. physica status solidi (a), 2004. **201**(6): p. 1302-1331.
13. Jurchescu, O.D., J. Baas, and T.T.M. Palstra, *Electronic transport properties of pentacene single crystals upon exposure to air*. Applied Physics Letters, 2005. **87**: p. 052102-1.
14. Koch, N., *Energy levels at interfaces between metals and conjugated organic molecules*. Journal of Physics: Condensed Matter, 2008. **20**: p. 184008.
15. Alves, H., et al., *Metallic conduction at organic charge-transfer interfaces*. Nature Materials, 2008. **7**: p. 574-580.
16. Mori, T., *Molecular materials for organic field-effect transistors*. Journal of Physics: Condensed Matter, 2008. **20**: p. 184010.
17. Kitamura, M. and Y. Arakawa, *Pentacene-based organic field-effect transistors*. Journal of Physics: Condensed Matter, 2008. **20**: p. 184011.
18. Reese, C. and Z. Bao, *Organic single-crystal field-effect transistors*. Materials Today, 2007. **10**(3): p. 20-27.
19. Horowitz, G., *Organic thin film transistors: From theory to real devices*. Journal of Materials Research, 2004. **19**(7): p. 1946-1962.
20. Dimitrakopoulos, C.D. and D.J. Mascaró, *Organic thin-film transistors: A review of recent advances*. IBM Journal of Research and Development, 2001. **45**(1): p. 11-27.
21. Hoffman, R.V., *Organic Chemistry: An Intermediate Text*. 2004, New Jersey: John Wiley & Sons, Inc.
22. Pope, M. and C.E. Swenberg, *Electronic Processes in Organic Crystals and Polymers*. 2nd ed. 1999, New York: Oxford University Press.
23. Shirakawa, H., et al., *Synthesis of electrically conducting organic polymers: halogen derivatives of polyacetylene, (CH)_x*. Journal of the Chemical Society, Chemical Communications, 1977. **16**: p. 578-580.

24. Bowden, M.J., *Electronic and Photonic Applications of Polymers*, ed. M.J. Bowden and S.R. Turner. 1988, Washington D.C.: American Chemical Society.
25. Knoester, J. and M. Mostovoy, *Disorder and Solitons in Trans-Polyacetylene*, in *Semiconducting Polymers: Chemistry, Physics, and Engineering*, G. Hadziioannou and P.F.v. Hutten, Editors. 2000, WILEY-VCH Verlag GmbH: Weinheim.
26. Tilley, R.J.D., *Understanding Solids: The Science of Materials*. 2004, Wiltshire: John Wiley & Sons Ltd.
27. Karl, N., et al., *Fast electronic transport in organic molecular solids?* Journal of Vacuum Science & Technology A, 1999. **17**(4): p. 2318-2328.
28. Jurchescu, O.D., *Molecular Organic Semiconductors for Electronic Devices*, in *Solid State Chemistry of the Materials Science Center*. 2006, Rijksuniversiteit Gronigen: Groningen.
29. Butko, V.Y., et al., *Field-effect transistor on pentacene single crystal*. Applied Physics Letters, 2003. **83**(23): p. 4773-4775.
30. Takeya, J., et al., *Field-induced charge transport at the surface of pentacene single crystals: A method to study charge dynamics of two-dimensional electron systems in organic crystals*. Journal of Applied Physics, 2003. **94**(9): p. 5800-5804.
31. Goldmann, C., et al., *Hole mobility in organic single crystals measured by a "flip-crystal" field-effect technique*. Journal of Applied Physics, 2004. **96**(4): p. 2080-2086.
32. Jurchescu, O.D., J. Baas, and T.T.M. Palstra, *Effect of impurities on the mobility of single crystal pentacene*. Applied Physics Letters, 2004. **84**(16): p. 3061-3063.
33. Mattheus, C.C., et al., *Identification of polymorphs of pentacene*. Synthetic Metals, 2003. **138**: p. 475-481.
34. Roberson, L.B., et al., *Pentacene Disproportionation during Sublimation for Field-Effect Transistors*. Journal of American Chemical Society, 2005. **127**: p. 3069-3075.
35. Yasuda, T., et al., *Ambipolar pentacene field-effect transistors with calcium source-drain electrodes*. Applied Physics Letters, 2004. **85**(11): p. 2098-2100.
36. Minari, T., T. Nemoto, and S. Isoda, *Fabrication and characterization of single-grain organic field-effect transistor of pentacene*. Journal of Applied Physics, 2004. **96**(1): p. 769-772.

37. Mills, W.H. and M. Mills, *The synthetical production of derivatives of dinaphthanthracene*. Journal of the Chemical Society, Transactions, 1912. **101**: p. 2194-2208.
38. Allen, C.F.H. and J. J.W. Gates, *A New Synthesis of the Pentacene Ring System*. Journal of American Chemical Society, 1943. **65**: p. 1502-1503.
39. Yamada, H., et al., *Photochemical Synthesis of Pentacene and its Derivatives*. Chemistry - A European Journal, 2005. **11**: p. 6212-6220.
40. Campbell, R.B., J.M. Robertson, and J. Trotter, *The Crystal and Molecular Structure of Pentacene*. Acta Crystallographica, 1961. **14**: p. 705.
41. Mattheus, C.C., et al., *Polymorphism in pentacene*. Acta Crystallographica, 2001. **C57**: p. 939-941.
42. Someya, T. *Research Projects : 有機分子の新物性探索*. 2004 [cited 2009 September 15th]; Available from: http://www.ntech.t.u-tokyo.ac.jp/Research/Research_project/Research_project_single_crystal/Research_project_single_crystal.html.
43. Endres, R.G., et al., *Structural and electronic properties of pentacene molecule and molecular pentacene solid*. Computational Materials Science, 2004. **29**(3): p. 362-370.
44. Jurchescu, O.D., et al., *Interface-Controlled, High-Mobility Organic Transistors*. Advanced Materials, 2007. **19**: p. 688-692.
45. Parisse, P., S. Picozzi, and L. Ottaviano, *Electronic, morphological and transport properties of 6,13-pentacenequinone thin films: Theory and experiments*. Organic Electronics, 2007. **8**: p. 498-504.
46. Koch, N., et al., *Molecular orientation dependent energy levels at interfaces with pentacene and pentacenequinone*. Organic Electronics, 2006. **7**: p. 537-545.
47. Vollmer, A., et al., *The effect of oxygen exposure on pentacene electronic structure*. European Physical Journal E, 2005. **17**: p. 339-343.
48. Conrad, B.R., et al., *Effect of impurities on pentacene island nucleation*. Physical Review B, 2008. **77**(20): p. 205328-1.
49. Bommel, G.v., *Sublimation of 6,13-pentacenequinone from pentacene single crystal surfaces*, in *Faculty of Science and Technology, Inorganic Materials Science*. 2009, University of Twente: Enschede.

50. Veen, P.d., *Unpublished work*. 2008.
51. Mott, N.F. and R.W. Gurney, *Electronic Processes in Ionic Crystals*. 2nd ed. 1948, Oxford: The Clarendon Press.
52. Zuleeg, R. and P. Knoll, *Space-Charge Limited Currents in Heteroepitaxial Films of Silicon Grown on Sapphire*. Applied Physics Letters, 1967. **11**(6): p. 183-185.
53. Boer, R.W.I.d., et al., *Space charge limited transport and time of flight measurements in tetracene single crystals: A comparative study*. Journal of Applied Physics, 2004. **95**(3): p. 1196.
54. Podzorov, V., et al., *Single-crystal organic field effect transistors with hole mobility ~ 8 cm²/V s*. Applied Physics Letters, 2003. **83**(17): p. 3504.
55. Käfer, D., et al., *Packing of Planar Organic Molecules: Interplay of van der Waals and Electrostatic Interaction*. Crystal Growth & Design, 2008. **8**(8): p. 3053-3057.
56. Jurchescu, O.D. and T.T.M. Palstra, *Crossover from one- to two-dimensional space-charge-limited conduction in pentacene single crystals*. Applied Physics Letters, 2006. **88**: p. 122101-1 - 122101-3.
57. Mattheus, C.C., *Polymorphism and electronic properties of pentacene*, in *Solid State Chemistry of the Materials Science Center*. 2002, Rijksuniversiteit Groningen: Groningen.